ALMA MATER STUDIORUM - UNIVERSITÀ DI BOLOGNA

SCHOOL OF ENGINEERING AND ARCHITECTURE

DEPARTMENT OF INDUSTRIAL ENGINEERING

SECOND CYCLE DEGREE IN ENERGY ENGINEERING

MASTER`S THESIS

in

Sustainable Technologies for Energy Resources

THE HAZARD OF DEFLAGRATION TO DETONATION TRANSITION FOR HYDROGEN-METHANE MIXTURE IN UN-OBSTRUCTED PIPELINES

Submitted by:
Enrico Tampieri

Supervisor:
Prof. Ernesto Salzano

Co-Supervisors:
Dott. Arnas Lucassen
Dott. Stefan Spitzer

Academic Year 2021/2022
Session III

ABSTRACT

In the transition to carbon neutrality, the addition of hydrogen to the gas grid is a key step toward reducing greenhouse gas emissions by partially replacing methane. Hydrogen is considered an important energy carrier and its introduction into the gas distribution pipelines does not require significant changes in the existing infrastructure.

The advantages of hydrogen as a carbon-free energy carrier have to be balanced against concerns about the safety of blended gas during transport, such as overpressure and leakage in pipelines, which under specific conditions can lead to the phenomenon of detonation. This step responsible to lead the mixture from deflagration to detonation is the main topic of the current study and it is better known as the deflagration-to-detonation transition (DDT).

Over the years, many experiments have been performed to study the safety characteristics of hydrogen/methane mixtures and the properties of DDTs, but none of them has ever been conducted in an unobstructed circular steel tube with a diameter of 5 cm. For this reason, this configuration was chosen for the present work, aimed at detecting the exact probability of a DDT transition as a function of initial conditions such as absolute pressure and hydrogen and methane concentrations. The initial pressure was varied from 1.1 to 2 bar, while the fuel fraction was varied from 100% H_2 to 100% CH_4, always maintaining the equivalence ratio λ to 1. To this end, six photodiodes and six piezoelectric sensors were installed along the tube, and a high-voltage induction spark was used as the ignition source.

It has been observed that the transition from deflagration to detonation occurs mainly around values of 80% hydrogen and that an increase in pressure leads to a lower hydrogen/methane ratio capable of detonating in unobstructed pipes. These and many other results are detailed in this work.

The investigations in this work can be a starting point for various experiments to obtain experimental data on pipe diameters, initial pressures, runup distances, and hydrogen/methane fractions for safety measures and calculations of possible DDT. In this paper, an initial comparison is presented between experiments carried out in a closed tube and an open one, under the same initial conditions.

TABLE OF CONTENTS

LIST OF FIGURES

LIST OF TABLES

INTRODUCTION

Over the years, the need for reliable and clean energy sources has increased dramatically. There are several reasons for this, the reduction of greenhouse gas emissions being the most important, as the problem of global warming has become something that can no longer be underestimated in the last years. The temperatures recorded in Europe during the current winter once again highlight the need for immediate action, and the substitution of methane as the main energy source is the first step towards achieving the emission reduction targets.

In addition to the reduction of greenhouse gases, there is the war involving Russia and Ukraine. This led to the disruption of Russian methane supplies to Europe, providing further motivation for immediate action in the search for new ways to produce energy without depending on Russian imports.

The most reliable and feasible of the known alternatives is to use the existing gas distribution lines built and reformed in recent decades, adding hydrogen to the methane mixture. In this way, CO_2 emissions will be reduced since the product of hydrogen combustion is water. For this reason, studies on hydrogen, and in particular on hydrogen-methane mixtures, have increased in recent years.

However, due to the large differences in properties between natural gas and hydrogen, many studies are needed to ensure the safety of these mixtures during production, storage and distribution, as well as to develop efficient end applications that can use hydrogen as a fuel.

Currently, the amount of hydrogen allowed in the mixture is limited to a maximum of 20 Vol% [1], and this is achieved using the same equipment and the existing gas network, while reducing overall carbon emissions.

Previously, the effects of hydrogen addition on the confined explosion were studied by Lowesmith et al. [2] as part of a project called NATURALHY. In their study, a series of large-scale explosion experiments were conducted with methane/hydrogen mixtures in a 69.3 m^3 enclosure to evaluate the effect of different mixture concentrations. The conclusions were that the addition of hydrogen up to 20 % by volume to air/methane mixtures resulted in a small increase in flame velocities and overpressures. However, a significant increase was observed when higher hydrogen concentrations were added.

The experiments were performed on systems of different shapes and sizes. Further experiments were also performed by Lowesmith [3] by adding a congested region of 3 m x 3 m x 18 m in length to the previous confined region [2]. The congestion consisted of 12 racks, spaced 1.5 m apart, alternately supporting 7 or 6 horizontal tubes, each 0.18 m long. Here one can see the effect of congestion and initial velocity and how these lead to a faster transition from deflagration to detonation (DDT). In fact, congestion and higher initial velocity increase both flame speed and overpressure when the H_2 concentration in the mixture reaches values of 40% or more.

A different structure was analysed by Shirvill et al. [4] in 2019. The system in question was a 3 m x 3 m x 2 m high facility containing nine layers of vertical grids in the lower half and seven layers of horizontal grids in the upper half. The researchers observed that the maximum overpressures generated by mixtures of methane and hydrogen with a hydrogen content of 25 per cent by volume or less are not likely to be higher than those generated by methane alone. Their work suggested that adding less than 25 per cent hydrogen by volume to pipeline networks would not significantly increase the risk of explosion.

Further experiments were performed in a spherical vessel by Qiuju et al. [5]. In the present work, a series of experiments was performed in a 20 L spherical vessel at initial conditions of 1 atm and 293 K, with methane-hydrogen/air mixtures at different concentrations. Temperature and pressure peaks were discovered, as it was observed that the temperature peak always lags behind the pressure peak upon arrival, regardless of fuel equivalence. Other important safety parameters were reported, such as the maximum pressure rise rate $(dP/dt)_{max}$ and minimum ignition energy. The maximum rate of pressure rise, together with the laminar burning velocity, were also quantified by Salzano et al. [6] for explosions of methane-hydrogen/air mixtures in a closed cylindrical steel vessel of 5 L volume.

DDT investigations of hydrogen-methane-air mixtures in a tube were conducted in 2013 by Porowski and Teodorczyk [7] and a few years later by Zhang et al. [8, 9] and Wang et al. [10]. The common aspect of these experiments is the presence of differently shaped obstacles within the tubes. Thus, an efficient randomisation of the flow through large-scale turbulence and wave reflections leading to DDT was achieved much earlier than with smooth tubes.

As a result of the experiment [7], the deflagration and detonation regimes and flame propagation velocities in the obstructed pipe were determined by placing pressure transducers along the pipe. The tube examined was a 6 m long circular section with an inner diameter of 140 mm and circular obstructions on the inside. In all these pipe experiments, the dimensions

of the detonation cells were measured using the smoked foil technique. In the article [9], published in the journal Fuel, good agreement was found between the experimental data and predictions based on a detailed chemical-kinetic model.

The setup of experiments [8] and [9] consisted of a 1.2 m long pipe with a 68 mm internal diameter steel drive section, followed by a 2.5 m long pipe test section with an internal diameter of 36 mm. The obstacles consist of an annular channel of different diameters placed within the test section.

The experiments [10] were conducted in a 6 m long square tube with an inner surface area of 112 mm x 112 mm. Stoichiometric mixtures of hydrogen-methane-air at ambient pressure (1 atm) and room temperature (293 K) were used and the obstacles consisted of square orifice plates distributed at various distances within the tube.

However, so far no experiments have been conducted on unclogged hydrogen-methane-air mixtures in ducts. What is presented in this work is something that can realistically represent the beginning of something new and useful in dealing with this special energy carrier such as hydrogen.

The present experiments are characterised by initial conditions very similar to those of the projects presented above, i.e. an ambient temperature of 293 K and an equivalence ratio of 1 for all tests. The initial pressure was varied from a minimum of 1.1 bar to a maximum of 2 bar, unlike most of the above experiments carried out with initial pressure conditions of 1 atm.

Many other studies have been conducted to better understand the properties of hydrogen-methane mixtures, which, as already mentioned, are different when compared to pure methane or pure hydrogen.

The flammability limits, especially the upper limit, have been the subject of many detailed studies. Indeed, as reported by Middha et al. [11] and Wierzba and Ale [12], the lower flammability limit of hydrogen/methane mixtures in air agrees well with Le-Chatelier's law. The dependence of the upper flammability limit on parameters such as temperature and fuel composition was also shown and a comparison between the experimental values and Le Chatelier's rule was provided.

Askar et al. [13] produced an overview of many safety characteristics of hydrogen/methane mixtures, showing how the dependence of these characteristics on the hydrogen fraction is mostly non-linear, while Chaumeix et al. [14] conducted experiments on auto-ignition delay times. In these experiments, many conditions, reagent concentration, equivalence ratio,

temperature and pressure were varied, and comparisons between experimental tests and simulation models were also shown.

In the paper produced by Cadorin et al. [15], it is shown how a commercial CFD code was used to evaluate pressure losses through pipes in a high-pressure gas flow and also the ability of CFD analysis to determine the energy performance of fuel transport in pipelines.

The phenomenon of deflagration-to-detonation transition (DDT) and the dimensions of detonation cells still present many obscure points that absolutely must be studied. Studies on the subject have been made since the 1980s with the article published by Bull, Elsworth and Shuff [16] and later by Ciccarelli et al. [17, 18], which paved the way for what could concretely save the world in the future.

The concept of blending hydrogen in existing natural gas networks has been investigated in many parts of the world. In particular, several long-term projects with trials of hydrogen-blending in small communities have been successfully conducted in Europe, while there have been fewer such projects in the United States, thus far [19]. The HyDeploy project is the UK`s first hydrogen blending deployment project that was initiated in 2019. The goal of the project is to blend 20 mol% of hydrogen in the current UK`s gas grid keeping the same end-use appliances while reducing overall carbon emissions. The aim is to reach net zero carbon emissions by 2050 under the UK Climate Change Act.

The experiments presented in this article are the beginning of a series of investigations aimed at obtaining experimental data on pipe diameters, initial pressures, runup distances and hydrogen/methane fractions for safety measures and calculations of possible DDT. It is hoped that the following will be a valuable contribution to the transition and achievement of carbon neutrality in the world.

1. SETUP

The study was performed in a 6.23 m long circular cross-section tube with an inner diameter of 50 mm. All the texted mixtures were stoichiometric hydrogen-methane-air mixtures with different species concentrations. The tube, made of steel, was closed on both sides when the experimental mixture was ignited. It was equipped with a high voltage induction spark as ignition source , the gas inlet on one side, and a relative humidity sensor and the outlet valve on the other. A temperature sensor was also added 0.45 m away from the outlet valve. In total six photodiodes and piezoelectric pressure sensors were installed at the positions displayed in Figure 1. An additional piezoresistive pressure sensor was added on the inlet side to adjust the beginning pressure. The tube was also equipped on the outside with a heating coat to always have a beginning temperature of 20 °C.

Different initial pressures were used, firstly 1.1 bar and afterwards increased to detect the behaviour of the mixture also for higher pressures, until a maximum of 2 bar. 1.1 bar is the minimum value of pressure allowed since decreasing it under this limit means operating to a lower value than the atmospheric pressure. There is no scientific interest in going under this value both because of the enormous amount of energy required to make the vacuum and because air inputs from outside must also be considered.

A total of 140 tests were conducted to obtain solid and reliable results, varying gas fractions and initial pressure, which means that around 70000 L of fuel mixtures were used during the investigations presented.

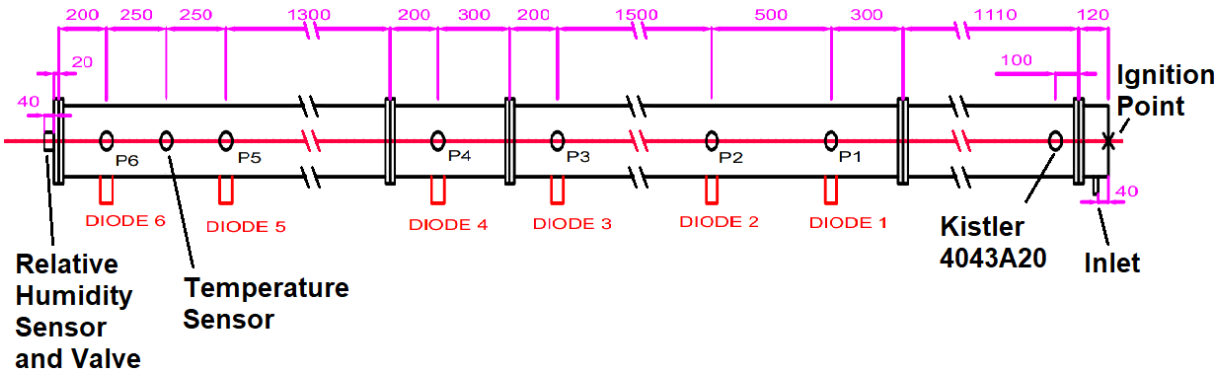

Figure 1 - Schematic of the setup used in this work for the DDT tests

1.1. KISTLER 4043A20 & MULTIMETER

The initial pressure was set constant through a multimeter connected to the pipe via a KISTLER 4043A20 piezoresistive transducer with a 500 mV/bar sensitivity. This device, shown in Figure 2, can measure the absolute pressure inside the pipe and read it on the multimeter monitor by simply doubling the voltage value (full range of 10 V/20 bar) (Figure 3). The measuring element in piezoresistive pressure sensors is a silicon Wheatstone bridge that extends minimally under pressure changing the electrical resistance, the pressure signal is in mV and it can be read on the display of a multimeter directly connected to the piezoresistive sensor through a cable.

Since the Kistler sensor measures the absolute pressure for the whole duration of the combustion, it is provided with a flame arrester which avoids the spreading of the flame toward the sensitive parts of the device (the piece with the yellow band in Fig.2). This is the only sensor featured with a flame arrester since it is the only one directly connected with the combustion inside the tube. All other sensors are not equipped with flame arresters, as diodes produce an optical measurement and are therefore not directly connected to the burning mixture, while piezoelectric sensors are equipped with a crystal coated with a protective membrane to measure the relative pressure. The coating protects the device from thermal shocks, especially at the beginning, because it may fail after several experiments, as seen in the section on defects and failures.

Figure 2 - KISTLER 4043A20 piezoresistive transducer

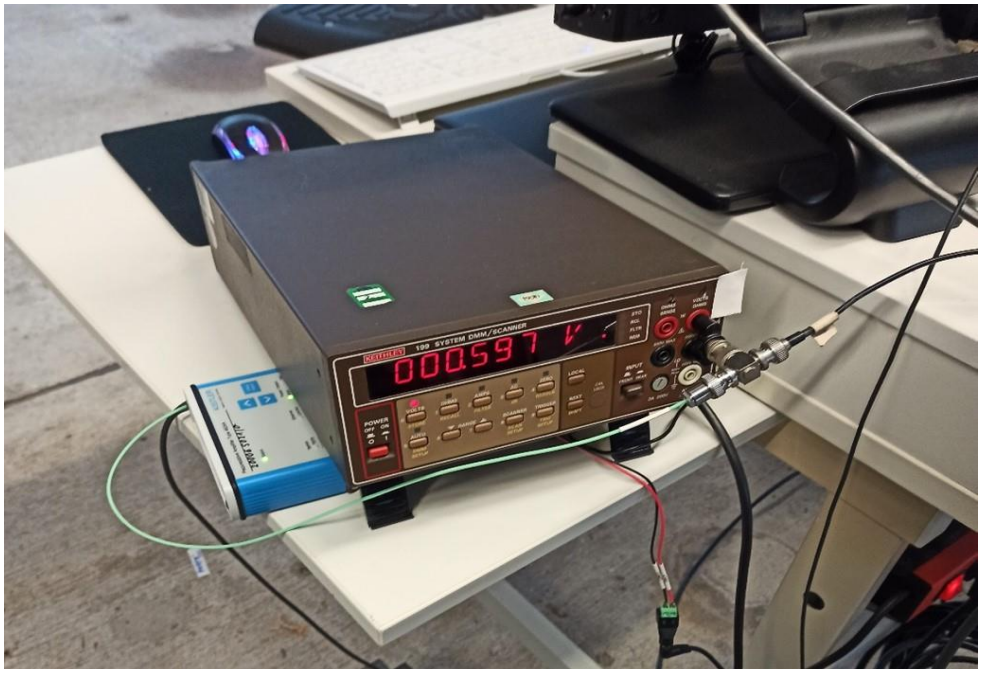

Figure 3 - Multimeter

1.2. PIEZOELECTRIC PRESSURE TRANSDUCERS PCB M102B03

The wave propagation was monitored by piezoelectric pressure transducers PCB M102B03 (Figure 4). Pressure transducers were located at different positions along the channel to collect data concerning DDT and detonation development. Sensors were placed separately along the tube, two at the beginning, two in the middle, and two at the end, spaced out 50 cm between each other. In this way, it had been possible to detect the transition behaviour along the whole pipe. These piezoelectric transducers measured relative pressure values during the combustion process, this means that when the pipe is open and there is no combustion inside, the values measured by these sensors are zero.

Indeed piezoelectric transducers are sensitive to dynamic changes and when a force is applied, an electric charge (Coulomb) is generated across the faces of a crystal material present inside the pressure sensor.

In the table below it is possible to see the name of each transducer, keeping in mind that the sensor's numeration starts from the ignition point, so number 1 is the closest to the electric spark while number 6 is to the end of the tube. (Table 1)

Figure 4 - PCB M102B03 piezoelectric transducer

Table 1 - Piezoelectric transducers PCB M102B03

Measuring range up to			70 bar	690 bar
Channel	Designation	Transducer	mV/bar	mV/bar
CH0	P1	SN-50841	7,356	7,283
CH1	P2	SN-50842	7,346	7,348
CH2	P3	SN-50843	7,393	7,353
CH3	P4	SN-50844	7,364	7,291
CH4	P5	SN-50846	7,205	7,145
CH5	P6	SN-50946	7,389	7,311

The two pressure values present in the upper table represent the maximum relative pressure values that can be measured by the system. In this case, 70 bar was acceptable, so the six sensors were calibrated according to the values listed in green. But what do these green values mean? The electric charge value coming from the piezoelectric transducer was then converted into a tension value through an amplifier, and then into a pressure value via a sensor box considering the relation mV/bar in green.

1.3. PHOTODIODES BPX65

Coupled with these devices, six photodiodes BPX65 were located along the tube and the values obtained were then used to calculate the flame speed. The six diodes were moved back 53 mm from the pipe's external surface to assure more precise results. This can be easily explained since the diodes detect the light intensity by providing a voltage measurement (mV), in this way, there is no interference with the light around the detection point. Photodiodes results were plotted in function of the time and the maximum capacity of these devices is 1 Volt.

Since the working principle of photodiodes is based on light radiation measurement, no direct contact with the combustion is involved and for this reason, no flame arresters are needed.

Table 2 lists all the diodes used for this experiment, keeping in count that Diode1 is the closest to the ignition point while Diode6 is the farthest.

Table 2 - Photodiodes

CH6	Diode1	1Volt
CH7	Diode2	1Volt
CH8	Diode3	1Volt
CH9	Diode4	1Volt
CH10	Diode5	1Volt
CH11	Diode6	1Volt

Figure 5 - Photodiode BPX65

1.4. BOX SENSORS AND AMPLIFIER

These devices were fundamental in processing the data and plotting the results. As explained earlier, piezoelectric sensor measurements were electric charge values that needed to be first amplified through an amplifier and then converted into pressure values.

In Figure 6 it's possible to see that for each pressure sensor there are two doors, one is an input and the next one is an output. Since these transducers produce an electric charge value (Coulomb), this is also the value given as input at the amplifier. In change, this device gives back a tension value in mV.

In the box sensors (black box in Figure 6), the conversion into pressure values occurred according to the green conversion values introduced in the piezoelectric pressure transducers section (Table 1). These values differ from sensor to sensor and are as precise as the maximum measurable value is lower.

The box sensors output is thus a pressure value (bar) plotted in function of the time.

For what concerns the photodiodes, they are directly connected to the box sensors through cables because their measured value doesn't need to be amplified.

Figure 6 - Amplifier

1.5. TEMPERATURE & RELATIVE HUMIDITY SENSORS

Two more sensors were placed at the end of the tube, the first one was a temperature sensor to check the value of the temperature inside the tube before the combustion. The second one was a relative humidity temperature meter to check the tube's relative humidity (red device). Both the results were then read on the devices' display and the humidity value was adjusted to conceded values before igniting the mixture. (Figure 7)

In Figure 8 it is possible to see the precise placement of the temperature sensor (grey metal wire and brown nut) which is exactly in the middle between the two piezoelectric transducers (blue wires), at a distance of 25 cm from each of them.

To adjust the humidity value, simply vary the opening of the valve that connects the sensor to the display to read the value (red device). The accepted range is up to a value of 5, so if the value is lower, it is possible to proceed with the next experiment, otherwise it is necessary to flush more air into the pipe.

These parameters were not taken into count for final evaluations since they were too flexible and different from trial to trial, depending on many factors and so not constant along the time.

As previously said, relative humidity was brought into a specific range before starting the ignition, just to homogenize the initial conditions as much as possible between each experiment, but no further considerations were done on these two parameters.

Figure 7 - Temperature and relative humidity sensors

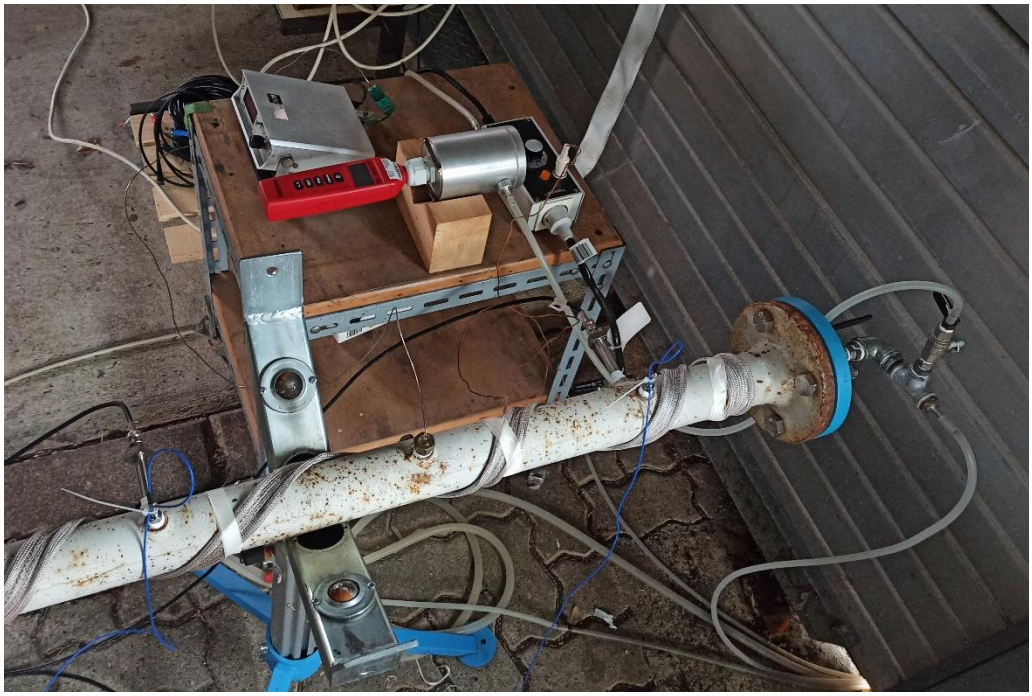

Figure 8 - Cables and devices disposition at the bottom of the tube

1.6. IGNITION SPARK

Texted mixtures were ignited by an electric spark at one end of the tube, more precisely in correspondence with the gas inlet. It is possible to see the ignition point in the figure below (Figure 9), more precisely where the red and black cables are located and connected to the red cage.

The order was given through an electronic-timer set at 0,5 sec, as shown in Figure 10. One of the main problems that affected our experiments was given by the voltage threshold set to generate the spark. In the beginning, this value was agreed to be 0 V but because of oscillations and vibrations causing auto-ignition and so the loss of data, this value was increased. Better explanations will follow in the section dedicated to defects and failures.

Figure 9 - Inlet side of the experimental system

Figure 10 - Electronic timer device

1.7. MIXTURE PREPARATION SYSTEM

The desired concentrations were set using a hand-held computer that could open or close the opening valve of each of the reagent flow controllers. Each of the tubes coming out of the air, hydrogen (UN 1049), and methane tank (UN 1971) was collected in a single tube connected to the pipeline inlet. It was in this intermediate pipe, about 5 meters long, that the mixture was pre-mixed, allowing for acceptable homogenization. (tank sizes)

The concentrations were typed in the software in form of percentages value and then transformed into a mass flow quantity.

Originally the total mass flow of the three species (methane, hydrogen, and air) was supposed to be 30 L/ min but because of the too big size of the hydrogen vessel, this value was doubled (60 L/min). In this way, better precision was assured. The hydrogen vessel was able to inject 50 L/min while the methane one 10 L/min, then increasing the flow meant asking for a lower accuracy to the mixture preparation system because more suitable quantities were needed according to the vessel size.

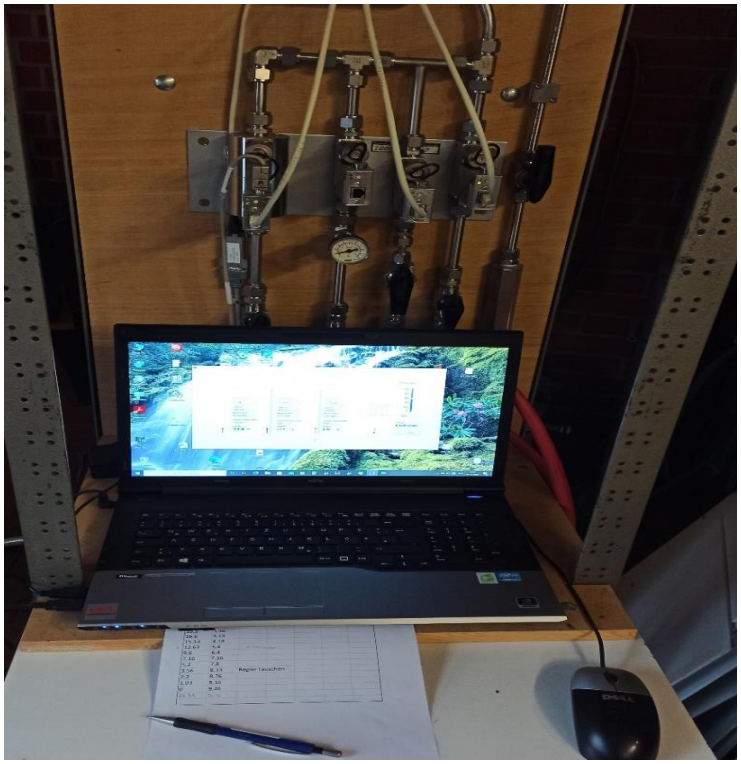

Figure 11 - Mixture preparation system

In the upper Figure 11, it is possible to see 5 tubes leaning on a wooden wall. The first one from the left was the air tube, the second one unused, and the third and the fourth respectively the hydrogen and methane tubes.

All these four tubes then converge in a single one and it is here that the pre-mixture starts. The external tube on the right is the continuation of the premixed one that then reaches the main pipe's inlet.

1.8. HEATING WIRE

To uniform initial and operational conditions as much as possible, the pipeline was wrapped up with a wires system device able to warm up the tube before starting experiments.

As is visible in Figure 12, this band of cables extends the entire length of the main tube and it is connected to a thermometer that compares the tube's temperature with the set value and warms the system up.

The tube temperature value is inserted between the two piezoelectric transducers close to the end of the tube.

Figure 12 – Heating wire

2. METHODS

In this section the right procedure followed to run experiments will be explained in detail as a sort of checklist.

2.1. PRE-COMBUSTION

Once every experiment was over, the next one was prepared fluxing air inside the pipe for at least 15 minutes, simply connecting the pre-mixing tube to the inlet and flowing only air (black tube (1) in Figure 13), in this way, the reaction products were expelled and the system was ready for the next experiment.

To reach a good degree of homogeneity and to allow the air to be thrown out, the premixed mixture was introduced and fluxed inside the system for 10 minutes before the next combustion. To do this the desired reactant quantities were typed into the specific laptop programme. This means that the volume is flushed approximately 50 times by the mixture for each experiment and considering that, a total of 140 tests were conducted, approximately 85000 L of fuel mixtures were used during the investigations presented.

During these 10 minutes of homogenization time, the right flow values were registered on the excel file and temperature and humidity were checked to be sure their values were not too different from the previous ones.

2.2. COMBUSTION PHASE

Once the 10 minutes of preparation time was over, the gas outlet valve was closed (n.1 in Figure 14), and the inlet mixture was still injected to rise the pressure inside the tube to a value higher than the one agreed upon for the initial conditions.

Meanwhile, the black and red wires were connected to the black and red cage. This is responsible for the spark generation. The two wires were disconnected after every experiment was over to avoid undesired ignition since the system was very sensitive to tension oscillations and perturbations.

Once the pressure was overtaken, the mixture composed of air, hydrogen, and methane was detached from the inlet (n.1 in Figure 13) and the valve was closed (n.4 in Figure 13). Successively, modulating the opening of a flow control device (n.3 in Figure 13), the pressure inside the tube was adjusted to the right value and then finally this last device was closed together with the red handle valve (n. 5).

Figure 13 - Inlet side

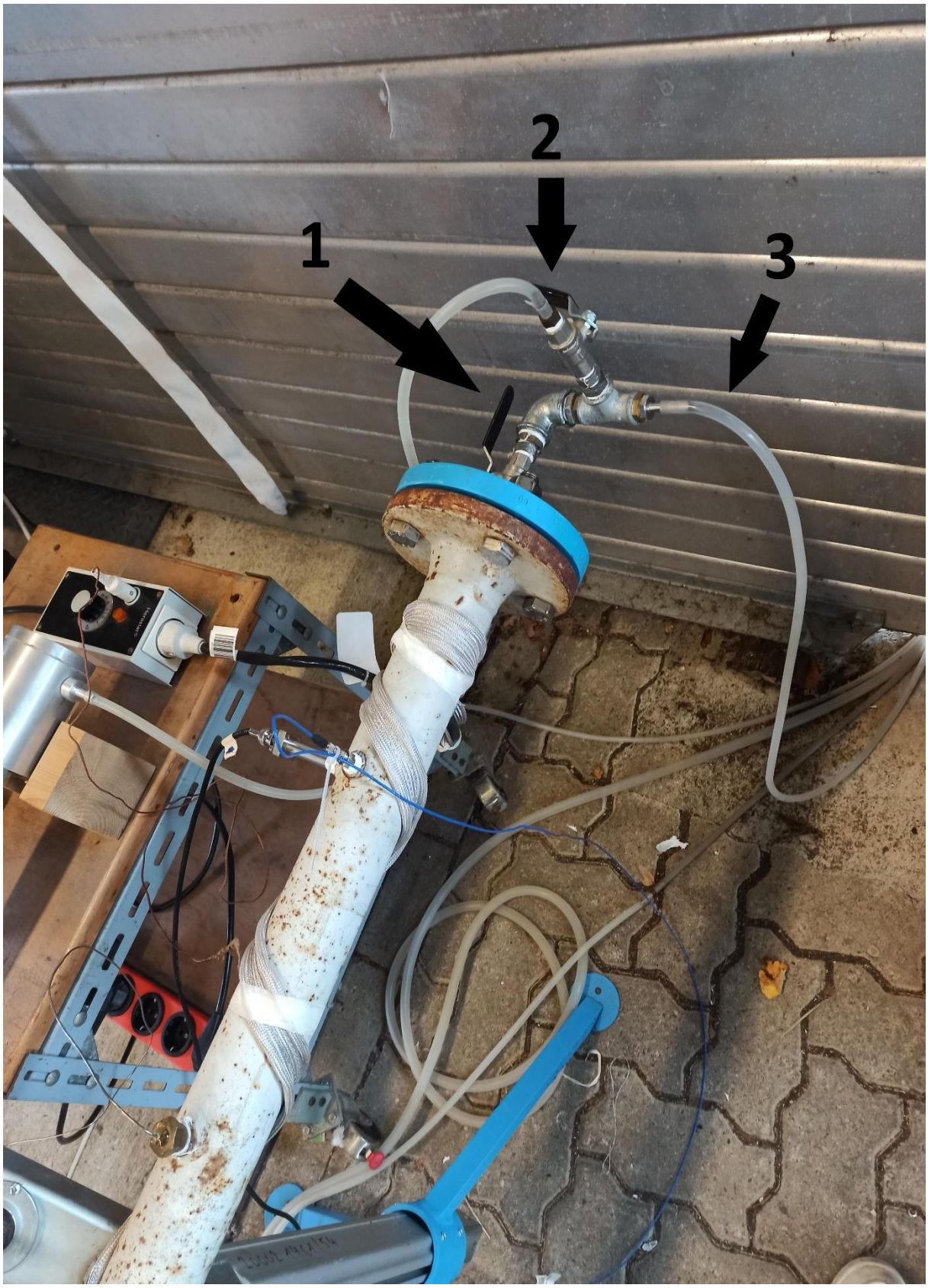

Figure 14 - Outlet side

Once all these steps were completed, the BENCH software was run and subsequently, the ignition spark button was pressed.

The BENCH software was essential to record all the data coming from piezoelectric transducers, the piezoresistive transducer and photodiodes and so mostly they were pressure and tension data related to the time value.

2.3. POST-COMBUSTION

The first step of the post-combustion phase was the air fluxing inside the tube to expel the combustion products and to prepare the new experiment.

This was achieved by opening valve number 1 in Figure 13 to let the flux leave the tube and at the same time opening valves 4 and 5 (Figure 12), previously closed to assure the right value of pressure inside the tube.

Once all these steps were completed, the black tube (n.1) was reconnected to the inlet, so that only air could be fluxed inside, and the red and black cables of the spark injection system were detached from the cage to avoid unexpected ignition.

All the steps followed were the same either in case of deflagration or detonation. Obviously during the combustion process was possible to guess which of the two phenomenons happened inside the pipe simply by paying attention to the generated noise.

The last step in the entire procedure was the saving of data via ASCII (.txt) and BENCH6 (.sb6dat) to enable better data management with the Origin software.

3. DATA AND CALCULATIONS

This chapter will explain how the calculations were performed. The values obtained were used during each experiment to specify the desired composition of the mixture, simply by entering the desired percentage of CH_4 and H_2 into the hand-held computer (Figure 10) (Table 3 columns % CH_4 and % H_2).

Once the exact percentages were entered, the system was able to provide the exact reagent flow at the inlet considering a total volumetric flow of 60 L/min. This means that approximately 600 L of mixture was used for each experiment, given a preparation time of 10 minutes.

Below it is possible see the two reactions on which all calculations are based. The first is the hydrogen combustion reaction (1), while the second is the methane combustion reaction (2).

$$H_2 + \frac{1}{2}O_2 \rightarrow H_2O \quad (1)$$

$$CH_4 + 2O_2 \rightarrow 2H_2O + CO_2 \quad (2)$$

By identifying the hydrogen content of the mixture with X, it was possible to calculate the volume of O_2 required to satisfy the stoichiometry of the reactions indicated above.

An important fact underlying each experiment is the equivalence ratio λ. In fact, since it was considered the most dangerous of cases, λ was chosen as 1. This means that the fuel and air in the mixture are in a perfect stoichiometric ratio and thus the best possible conditions for successful combustion.

Therefore, considering the amount of H_2 and CH_4 in the two reactions, the calculation to determine the volume of O_2 for a stoichiometric reaction is given below.

$$\frac{X}{2} + 2(1 - X) = 2 - \frac{3}{2}X \quad (3)$$

Once the volume of O_2 has been determined, to calculate the correct volume of air for a stoichiometric reaction (Table 3 column "Air"), simply divide the value just found above by the exact percentage of O_2 normally present in the air composition.

$$\text{Air volume:} \quad \frac{2-\frac{3}{2}X}{0.20942} \tag{4}$$

The last three columns contain the values to be entered into the computer according to the desired concentration. They were obtained simply by converting the volume of CH_4, H_2 and Air to a percentage value in relation to the total volume of the mixture (Table 3 column "Mixture").

The CH_4 fraction and the H_2 fraction were chosen in this way, considering that the transition from deflagration to detonation occurs mainly around values of 0.2 methane fraction.

Table 3 - Data used

CH_4 fraction	H_2 fraction	O_2	Air	Mixture	% CH_4	% H_2	% Air
per L	per L	per L of Fuel	per L of Fuel	per L of Fuel	per L of Mixture	per L of Mixture	per L of Mixture
(1-0)	(0-1)	m^3	m^3	m^3	%	%	%
1	0	2	9,5502	10,5502	9,48	0,00	90,52
0,9	0,1	1,85	8,8339	9,8339	9,15	1,02	89,83
0,8	0,2	1,7	8,1177	9,1177	8,77	2,19	89,03
0,7	0,3	1,55	7,4014	8,4014	8,33	3,57	88,10
0,6	0,4	1,4	6,6851	7,6851	7,81	5,20	86,99
0,5	0,5	1,25	5,9689	6,9689	7,17	7,17	85,65
0,4	0,6	1,1	5,2526	6,2526	6,40	9,60	84,01
0,3	0,7	0,95	4,5363	5,5363	5,42	12,64	81,94
0,25	0,75	0,875	4,1782	5,1782	4,83	14,48	80,69
0,225	0,775	0,8375	3,9991	4,9991	4,50	15,50	80,00
0,2	0,8	0,8	3,8201	4,8201	4,15	16,60	79,25
0,175	0,825	0,7625	3,6410	4,6410	3,77	17,78	78,45
0,15	0,85	0,725	3,4619	4,4619	3,36	19,05	77,59
0,1	0,9	0,65	3,1038	4,1038	2,44	21,93	75,63
0	1	0,5	2,3875	3,3875	0,00	29,52	70,48

4. RESULTS AND DISCUSSION

4.1. PROBABILITY OF DETONATION

This chapter will present and discuss the graphs and results observed. As mentioned above, a total of 140 tests were performed throughout the entire experiment and all of them were carried out by changing parameters such as initial pressure and mixture concentration. On the other hand, some values were kept constant throughout the entire procedure. In fact, the ambient temperature was around 20 °C and the equivalence ratio λ was 1. All the performed tests are visible in Appendix A.

The initial pressure values varied between a minimum of 1.1 bar and a maximum of 2 bar, while the mixture concentration varied from pure hydrogen to pure methane. As the main objective of the subject was to detect the transition from deflagration to detonation, most of the tests were performed in the range between zero and 30 per cent methane, as the tipping point lay between these values.

A tipping point is defined as the exact point on the graph where no detonations occurred, which means that the set of tests performed under those specific conditions did not present detonations but only deflagrations.

The probability of a transition to a DDT is shown in Figure 15. It can be clearly seen that the increase in pressure results in a higher possibility of DDT. For a pressure value above 1.5 bar, the tipping point is constant between 22.5 % and 25 % methane, while for lower pressure values, the tipping point linearly decreases to values of 20 % and 22.5 % methane.

Indeed, for the above mentioned 20 % fraction of methane, considering an initial pressure of 1.1 bar, one of the four tests showed DDT, while increasing it only slightly showed no sign of DDT. By decreasing it slightly, the possibility increases considerably.

An estimate as to what combination of pressure-ratio-length of methane and hydrogen a DDT might occur, especially for the permitted quantities that are currently present in gas networks, will be established and presented with further tests.

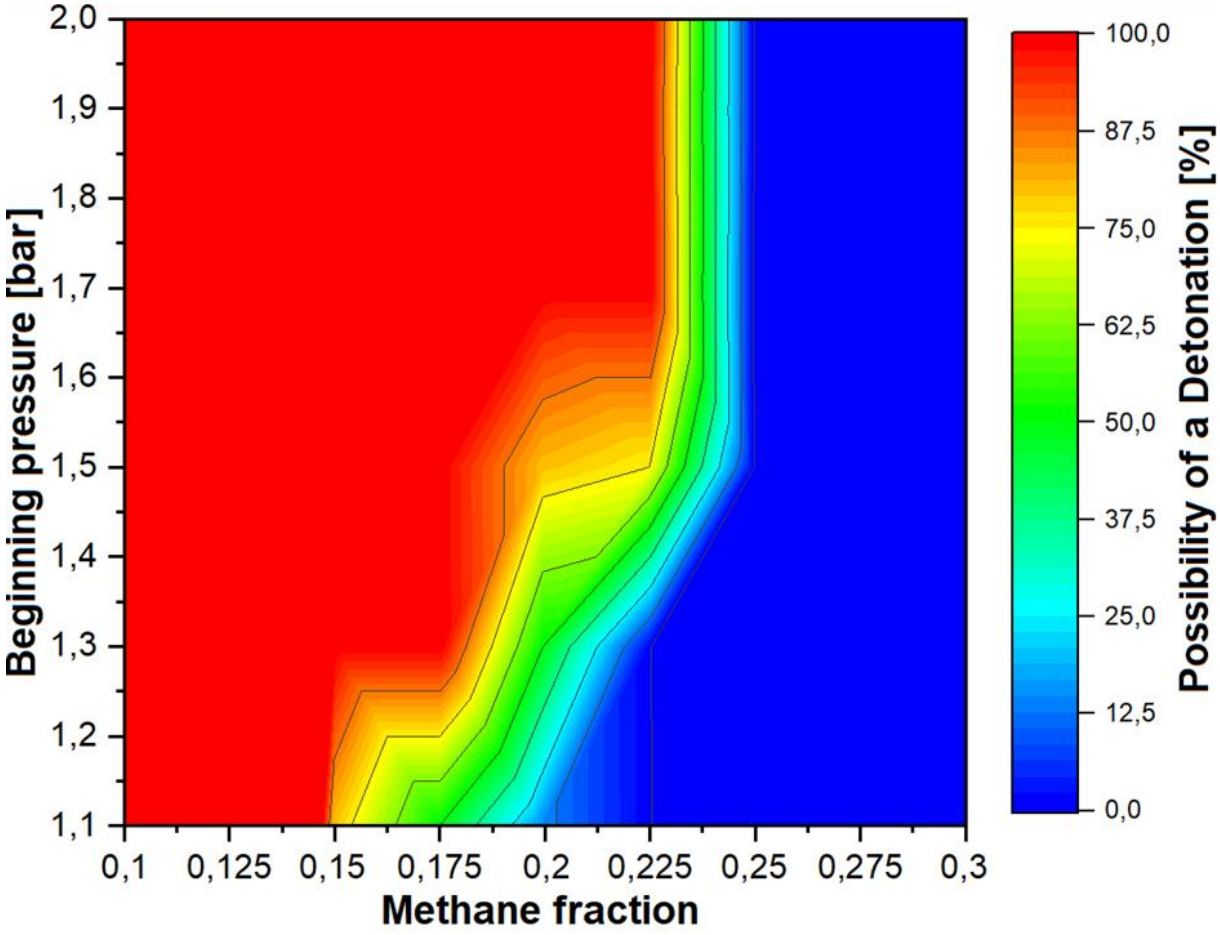

Figure 15 - Influence of pressure on the possibility of the hydrogen-methane-air mixture to a DDT

4.2. PHOTODIODES DATA

In this paragraph are shown graphs obtained by data recorded from photodiodes during the experiment. In Figure 16 is presented the DDT occurred for TEST 115 and so 0,175 methane fraction and pressure 1,1 bar while in Figure 17 is possible to see the deflagration registered for TEST 116 characterised by 0,2 methane fraction and initial pressure 1,1 bar.

It`s possible to see the different voltages registered for the two different cases, by photodiodes with a capacity of 1 Volt. Through this voltage measurements it had been possible calculating the flame velocity of the mixture inside the pipe.

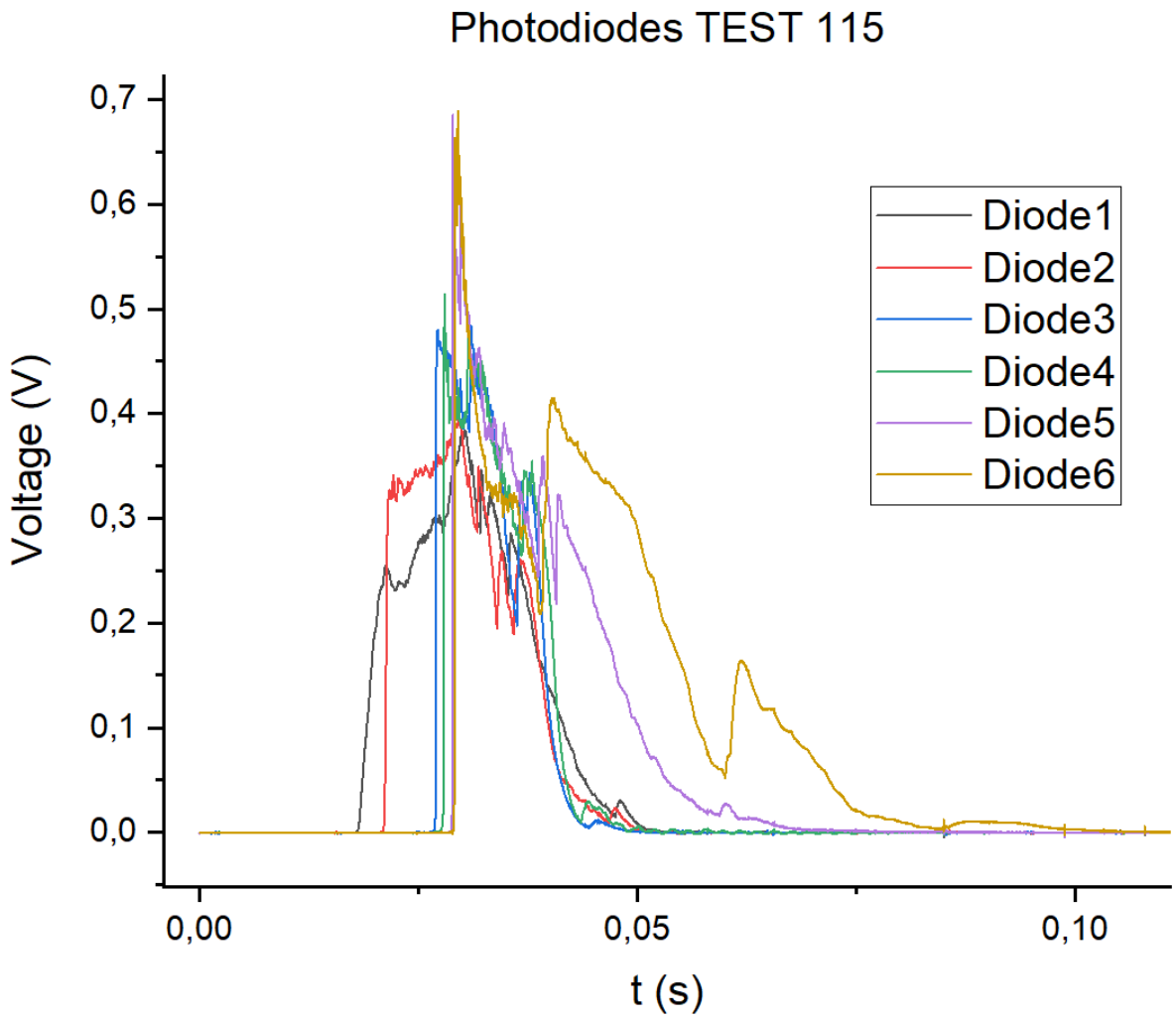

Figure 16 - Photodiode data for TEST 115 (0,175 methane fraction; initial pressure 1,1 bar)

To do that an y value was fixed. The most important requirement for the choice of this value was that each diode had to overtake this voltage threshold during the first rise of its curve.

In this way, knowing the time difference required from two following diodes to reach this fixed voltage value, and the space difference between these two following diodes (Figure 1), was possible, doing the ratio of these two quantities, to find the flame velocity of the mixture during the combustion.

Normally, y values used for these calculation, were 0.2 V for the tests where detonations occurred because they were further away from the 0 V line and 0,1 V in case of deflagration.

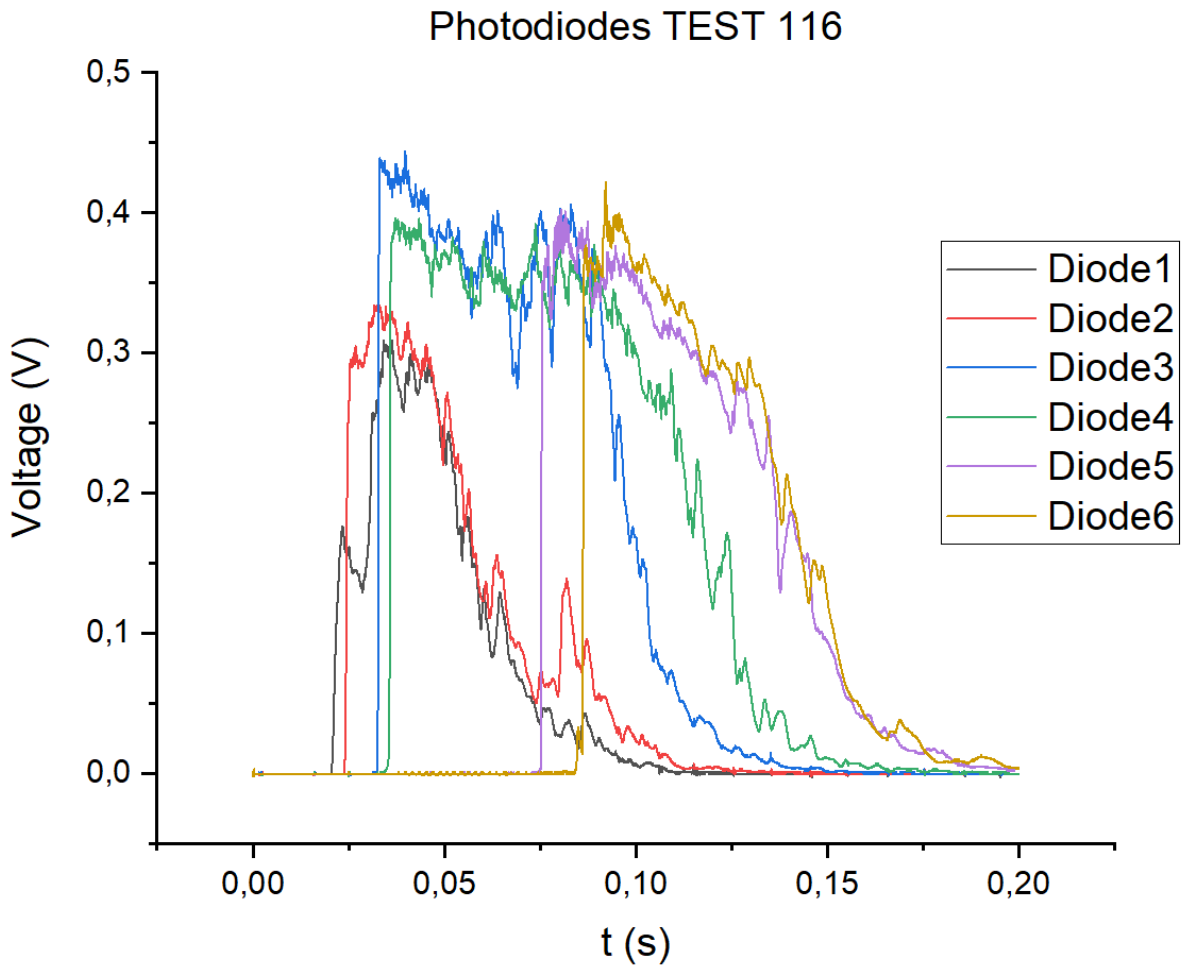

Figure 17 - Photodiode data for TEST 116 (0,2 methane fraction; initial pressure 1,1 bar)

4.3. VELOCITY PLOT – INITIAL PRESSURE 1,1 BAR

Figure 18 shows the measured flame speed for hydrogen-methane mixtures, ranging from pure hydrogen to 30 % methane, in the experimental tube described above. As mentioned above, velocity values were calculated using the voltage data recorded by the photodiodes.

Three regimes can be observed in all curves. After the initial deflagration regime, the flame first accelerates to a sonic regime at the burned gas temperature. Then, for low content of methane, a dramatic increase of the flame velocity up to the detonation regime is observed.

This is the case of freely propagating detonations, also known as Chapman-Jouguet (CJ) because of the sonic condition behind them. Because of the closed tube, the burnt gases, being at a higher temperature and pressure than the fresh gases, are able to generate pressure waves which, travelling at the speed of sound, overcome the flame front (which moves at subsonic

speeds) and compress the fresh gases they pass through, heating them and rising their pressure. This will result in the flame front finding warmer and warmer gases in its path and accelerating. This is the phenomenon at the base of Deflagration-to-Detonation Transition [21].

Figure 18 shows the flame speed graph for an initial pressure value of 1.1 bar. This is the lowest pressure value used in subsequent experiments. The velocities for methane concentrations of 0 % and 10 % reach a maximum at a distance of 478 cm from the ignition point. The situation is different for slightly higher methane fractions, since for methane concentrations between 15 % and 20 % the peak is not reached inside the tube.

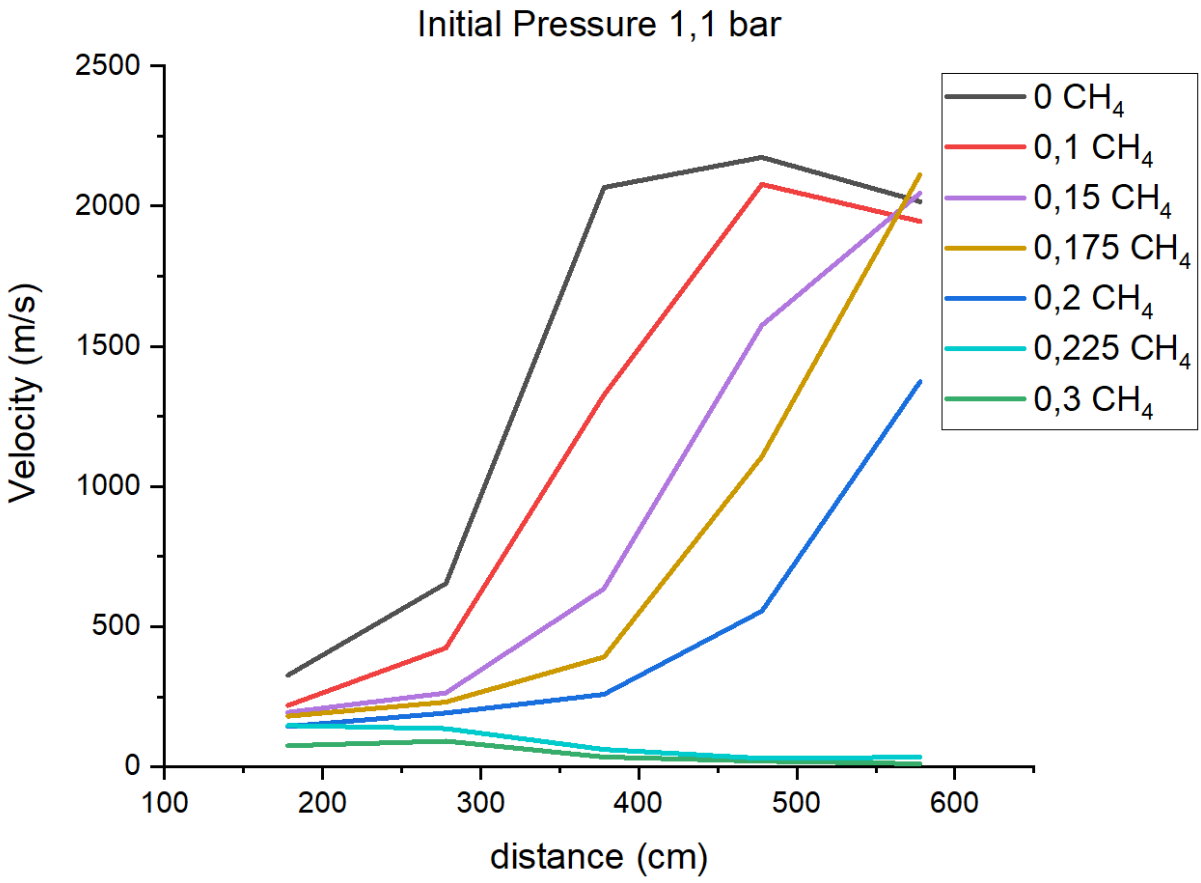

Figure 18 - Velocity plot for an initial pressure of 1,1 bar

An estimate of the exact distance at which the maximum flame velocity is reached can be made by looking at the C-J velocities in Table 4. These values were calculated using NASA software and in this way it is possible to estimate the maximum flame velocity reached by a mixture during its detonation process.

In fact, these values are around 2000 m/s, and since the velocities found at the end of the tube for mixtures with methane fractions of 15 % and 17.5 % were also around 2000 m/s, it can be assumed that the peak can be reached not far from the end of the tube, and therefore probably within 8 metres from the ignition spark.

The velocity values found in the experimental tests are slightly higher than those observed in Table 4. This is probably due to the compression wave and thus increasing pressure that results in higher flame velocities in the experimental case than in the simulations.

This shows the difference between these two ways of performing experiments, as the experimental one, unlike simulations, is subject to many unpredictable and uncontrollable factors.

Table 4 - Properties of the hydrogen-air mixtures analyzed in this work as calculated by CEA [20]. Initial pressure: 1.1 bar and 5 bar, at ambient temperature. Fuel at stoichiometric concentration (λ=1).

CH_4, $\%_v$	H_2, %	Initial Pressure (bar)	Sonic velocity at the burned gas temperature (m/s)	C-J (m/s)	Pressure (bar)
0	100	1.1	1090.4	1966.8	17.17
10	90		1062.2	1916.1	17.62
20	80		1044.3	1884.2	17.93
30	70		1032.1	1862.4	18.17
0	100	5.0	1111.1	1995.8	79.85
10	90		1081.4	1942.8	81.80
20	80		1062.7	1909.8	83.20
30	70		1050.0	1887.2	84.26

It is possible to observe, following on from what was mentioned above, the trend of the runup distance. This term refers to the length of the tube required to reach a critical flame velocity suitable for triggering the transition from deflagration to detonation. In other words, it can be considered as the point at which the flame velocity exceeds the speed of sound for combustion

gases. It is visible that it is shorter for low methane fraction (0 % and 10 %) since the highest speed has been reached within the tube, while is longer for higher methane concentration.

It can be said that the run-up distance, for a given pressure value, increases with increasing methane fraction.

Figure 18 also shows the already mentioned tipping point. It is clearly visible that, under these specific conditions, it lies between 20 % CH4 fraction and 22.5 % CH_4 fraction.

In fact, one of the four tests performed with a methane fraction of 20 % showed DDT, while increasing it only slightly showed no sign of DDT. Decreasing it slightly increases the possibility considerably.

As the experiment tube is closed, the products of combustion are responsible for generating a pressure stagnation. As a result of this pressurisation, it is possible to state that the actual pressure inside the tube during combustion is higher than the initial pressure setting.

Comparing the pressure values obtained through the simulations for an initial pressure of 5 bar and the relative pressure peaks recorded by the piezoelectric transducers during the experiments with an initial pressure of 1.1 bar, it can be seen that due to pressurisation, the pipe reached the adiabatic flame temperature for a pressure of approximately 5 bar. (Table 4) (Figure 19)

In fact, Figure 19 shows the relative pressure values for TEST 1 (0 % CH_4 – 100 % H_2 and initial pressure 1,1 bar) measured by the six piezoelectric transducers along the pipe. The highest value recorded by sensor 3 is approximately 68 bar. This is 10 bar lower than that recorded in the simulation for an initial pressure of 5 bar.

It is possible that the pressure peak during combustion was reached at another point in the pipe and not exactly at the six piezoelectric transducers. Another possibility could be that the pressure value reached due to pressurisation was not 5 bar, but somewhat lower.

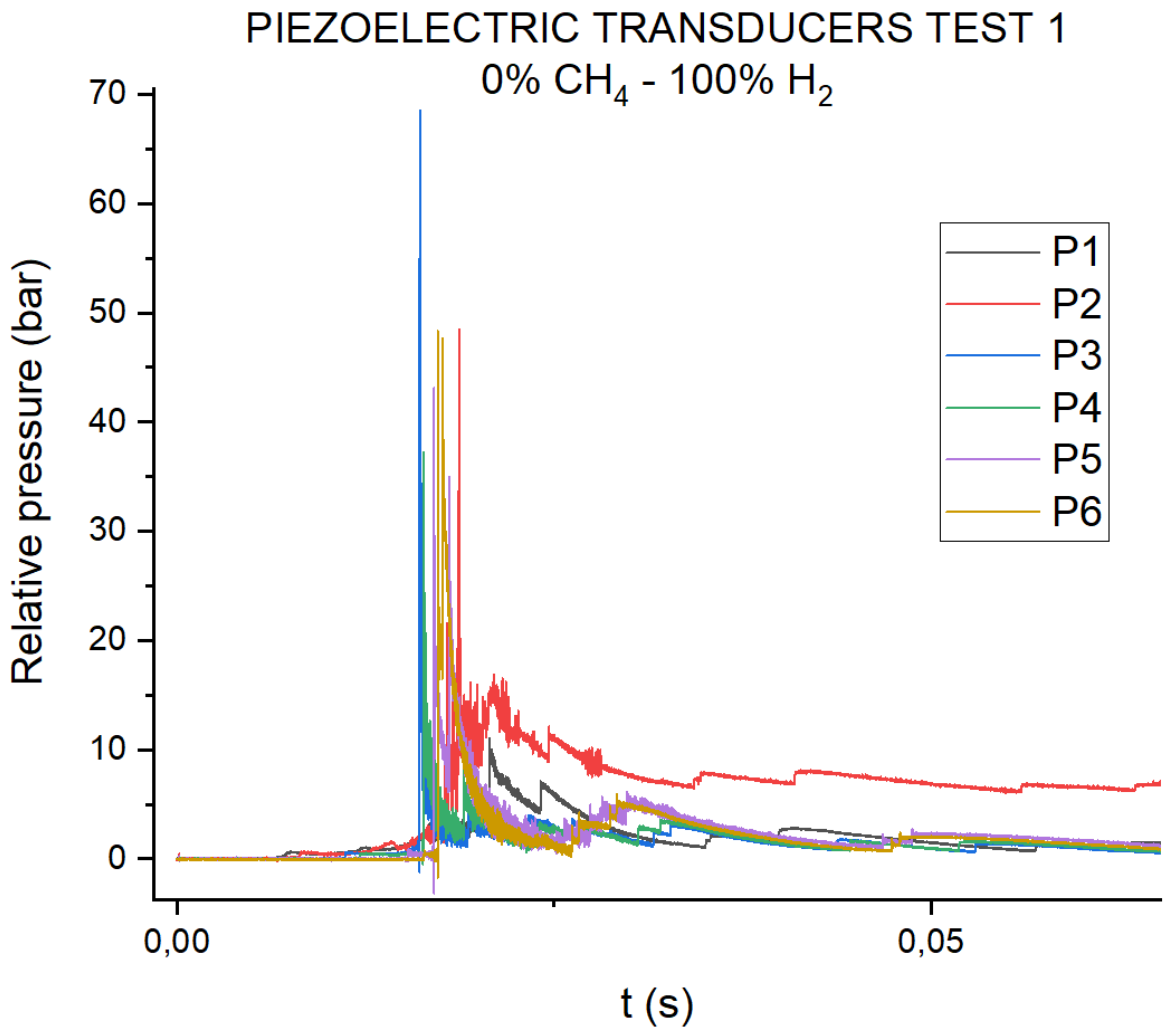

Figure 19 - Relative pressure values measured for TEST 1 (0 % CH_4 – 100 % H_2; 1,1 bar)

Another example is presented in Figure 20. Here, one can see the relative pressure values for TEST 2 (10 % CH_4 – 90 % H_2 and initial pressure 1,1 bar) recorded by the piezoelectric transducers. As for TEST 1, the highest measured value is approximately 10 bar lower than that obtained through simulations (Table 4).

The only difference is that in this case the peak and more in general the rise in pressure, were reached at sensor 5, instead of 3 as in the previous case. This is also visible looking at the time scale of the two graphs. This means that the distance between the ignition spark and the DDT (run-up distance) increases for higher methane fractions.

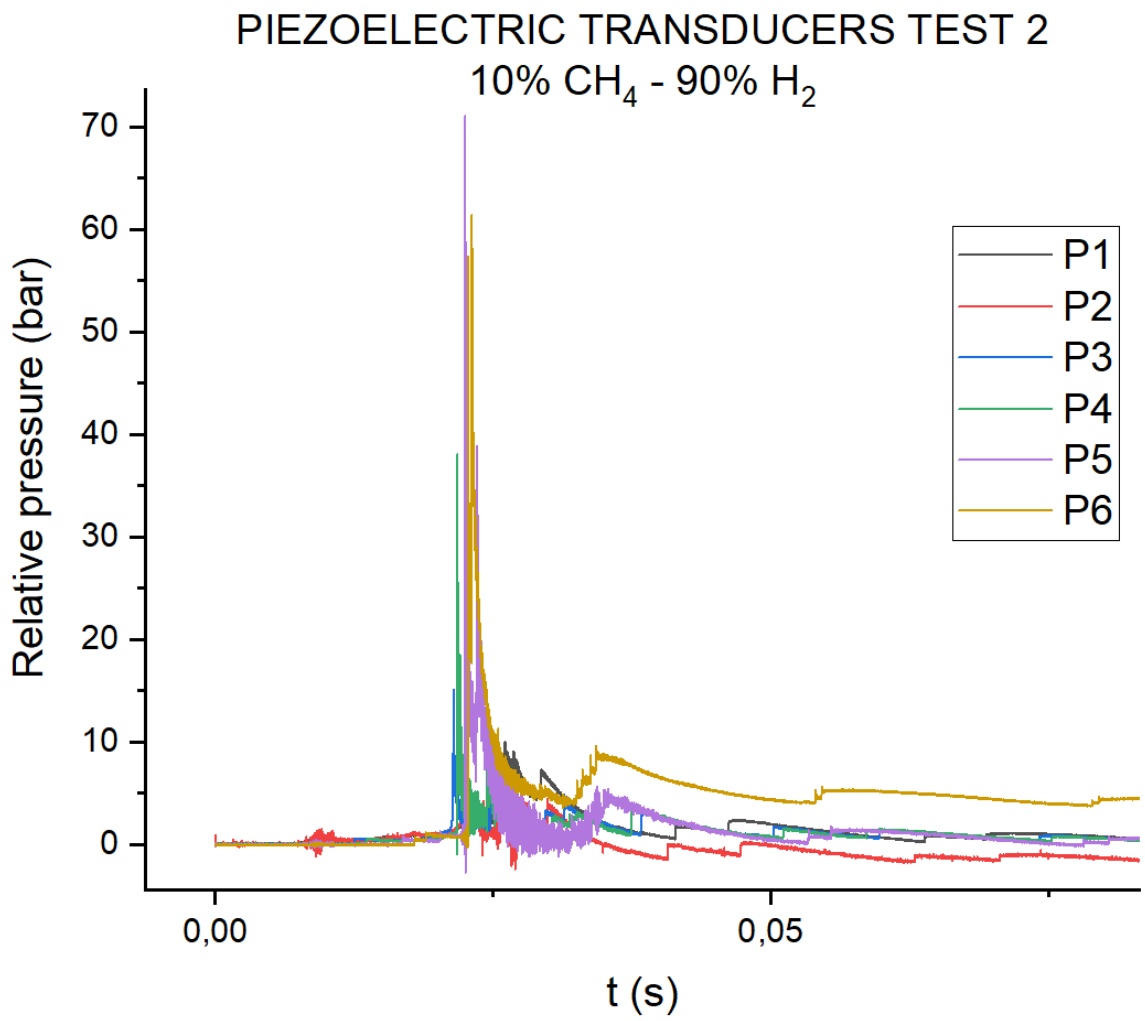

Figure 20 - Relative pressure values measured for TEST 2 (10 % CH_4 – 90 % H_2; 1,1 bar)

4.4. PRESSURE PLOTS ANALYSIS FOR 100 % H_2 AND 90 % H_2 AT 1,1 BAR

By observing and studying the pressure diagrams shown in Figure 19 and Figure 20, many aspects can be identified and understood, such as time interval and the approximate location where DDT and the detonation occurred.

Figure 21 shows the enlarged relative pressure graph for TEST 1. The DDT can be located where the relative pressure value overcomes the value of 5 bar. In fact, in cases where only deflagration is visible, the relative pressure plot is uniform around a value between 3 and 4 bars. For this reason, when a value higher than 5 bar is registered, it is possible to say that

DDT is occurring. In this case the transition is recorded at the same time than the highest pressure value, and so in correspondence with sensor 3 (353 cm from the ignition spark).

From this graph, it is not possible to state that the pressure peak lies between piezoelectric sensors 2 and 3 rather than between 3 and 4, but it is certainly in the vicinity of sensor number 3.

Checking the speed graphs that will be presented later (paragraph 4.5.), it can be seen that DDT occurs before sensor number 3 (353 cm from ignition) and then around 300 cm.

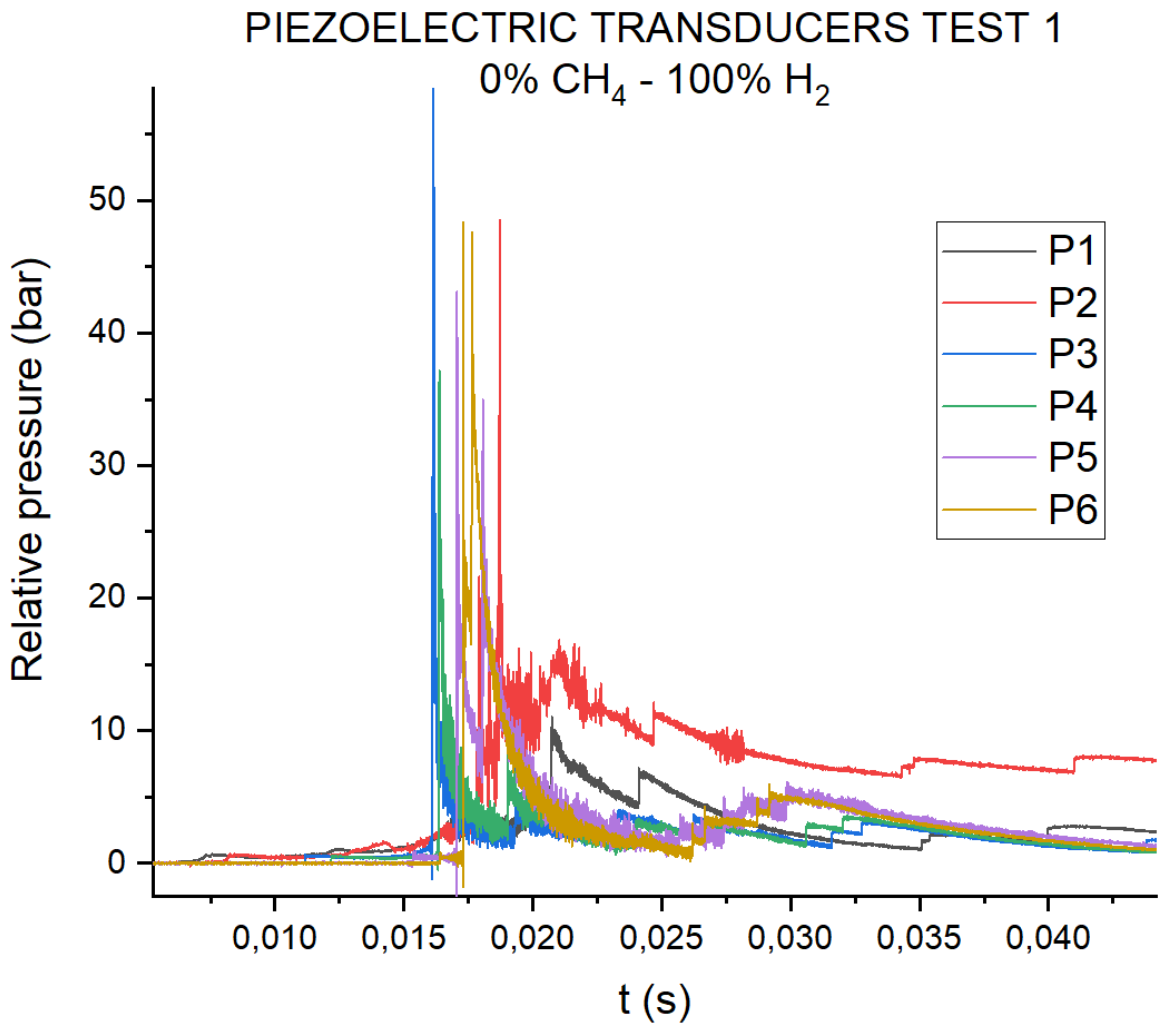

Figure 21 - Enlarged TEST 1 relative pressure plot (1,1 bar)

In Figure 21 it can be seen that two pressure waves propagate immediately after DDT, one in each direction of the tube. The one propagating in the same direction as the flame is recorded

by P5 and P6. It is reflected from the end of the tube with a similar intensity to the previous one (about 47 bar) and can be deduced from the fact that P6 has two peaks at a fraction of a time apart and then again in front of P5 but now with a lower intensity (35 bar).

The second original wave propagating after the detonation is recorded by P2 at about 0.019 s (about 47 bar), then ahead of P1 but with a sharp decrease in intensity as the peak is recorded at 10 bar.

This pressure wave reflection phenomenon continues over time with a gradual decrease in relative pressure intensity.

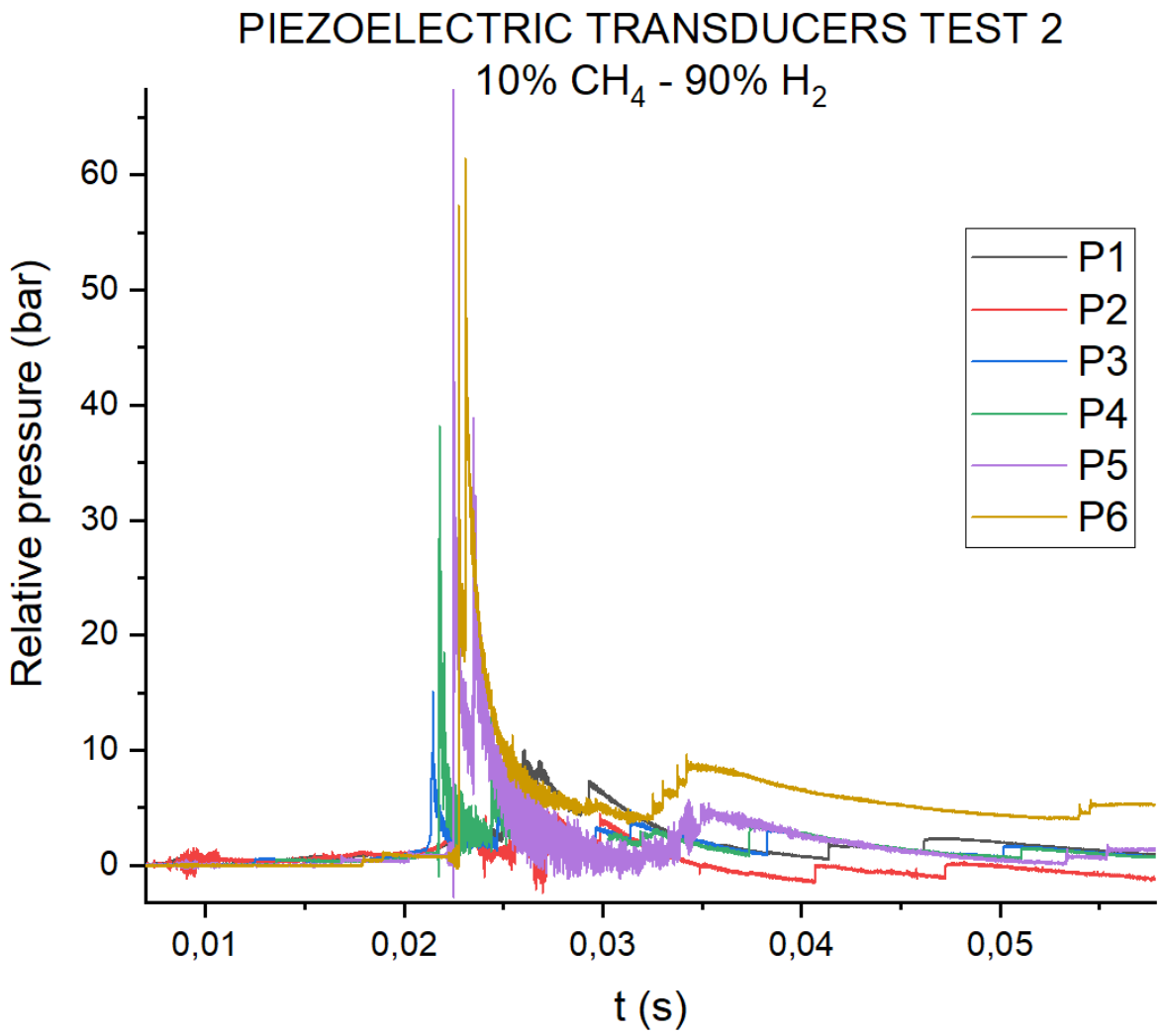

Figure 22 - Enlarged TEST 2 relative pressure plot (1,1 bar)

Figure 22 shows the relative pressure graph for TEST 2 (10 % CH_4 – 90 % H_2; 1,1 bar). This shows a peak at about 70 bar recorded by piezoelectric sensor number 5 (visible in Figure 20).

As with the previous test, looking at the current graph it is possible to assume that DDT occurs around sensor 3. This is confirmed by the speed diagram (paragraph 4.5.) where the flame speed exceeds the speed of sound between sensors number 3 and 4.

Also in this case, a pressure drop can be seen after the pressure peak is reached by looking at the trend of P6. Again, two pressure waves propagate in the two opposite directions of the tube.

The one proceeding towards the end of the pipe is reflected with an intensity of about 60 bar (P6) and abruptly decreases in intensity as it travels back down the pipe. Unfortunately, the course presented by the two different waves is not easily distinguishable due to the disturbed P5 wave partially hiding all other values.

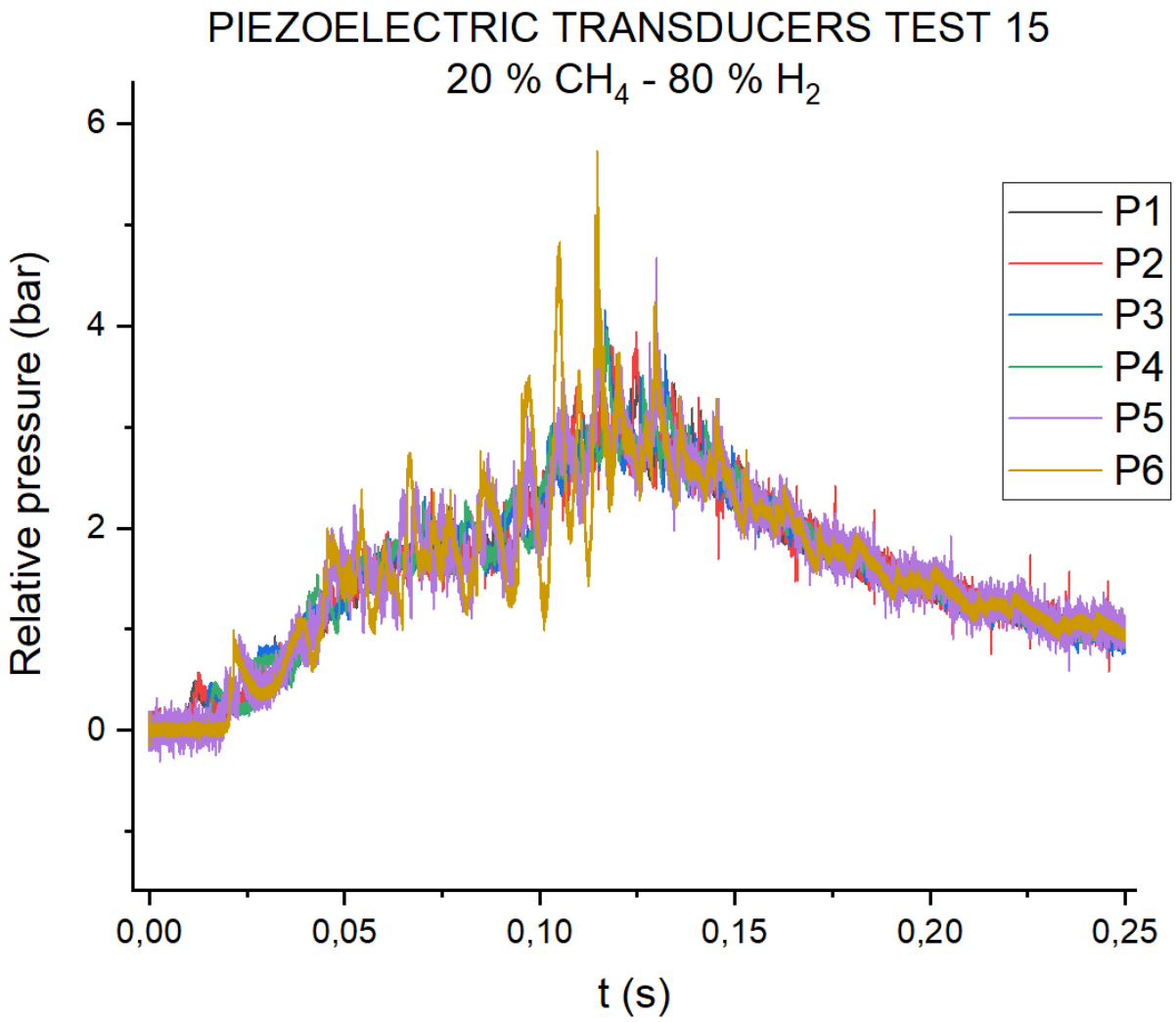

Figure 23 - TEST 15 relative pressure plot

Figure 23 shows a deflagration case for an initial pressure of 1.1 bar and 20 % CH_4 – 80 % H_2. The pressure values are lower and more uniform than in the case involving a DDT, waving around a value of 4 bar.

All other pressure diagrams presenting a DDT, show a relative pressure diagram similar to that shown for TEST 2, with a transition from deflagration to detonation further away from the ignition spark, when the methane fraction increases. In the next chapter, the prediction of a more accurate DDT will be presented by analysing the velocity diagrams.

4.5. COMPARISON BETWEEN DDT AND SOUND SPEED

In this chapter a comparison between velocity values obtained through photodiodes and mixture sound speeds is shown. It is known from the theory that the transition from deflagration to detonation occurs once the flame velocity overcomes the speed of sound for that specific mixture. So around this value, the deflagration reaches its maximum velocity prior to the transition to the detonation regime. Since there are numerous aspects that characterize DDT like turbulence and pressure waves, it is unlikely that any general theory can be developed to describe the phenomenon. What is shown in this chapter is an analysis of possible parallelisms and similarities found in the performed experiments.

Values presented in Table 5 have been obtained through a software named Gaseq. It allows to calculate adiabatic flame temperature keeping constant the pressure before and after the combustion. This means that the pipe used for this ideal simulation is an open pipe and that is the reason why values obtained below are different from the value presented in Table 4, where simulations were performed considering a closed tube with varying pressure, more similar to the current experiment.

Table 5 - Gaseq sound speeds considering ambient temperature T=293,15 K and stoichiometric ratio λ =1.

H_2	CH_4	PRESSURE	SOUND SPEED	
%	%	bar	Reactants (m/s)	Products (m/s)
100,0	0,0	1,1	404,0	1008,4
90,0	10,0	1,1	389,2	981,0
85,0	15,0	1,1	382,1	978,8
82,5	17,5	1,1	379,7	966,8
82,5	17,5	1,3	379,7	967,5
82,5	17,5	1,5	379,7	967,5
80,0	20,0	1,1	377,5	962,8
80,0	20,0	1,3	377,5	963,4
80,0	20,0	1,5	377,5	964,0
80,0	20,0	1,7	377,5	964,5
80,0	20,0	1,9	377,5	964,9
77,5	22,5	1,1	375,6	960,2
77,5	22,5	1,3	375,6	960,8
77,5	22,5	1,5	375,6	961,4
77,5	22,5	1,7	375,6	961,9
77,5	22,5	1,9	375,6	962,3
77,5	22,5	2,0	375,6	962,5
75,0	25,0	1,1	373,6	962,5
75,0	25,0	1,3	373,6	962,5
75,0	25,0	1,5	373,6	962,5
70,0	30,0	1,1	370,3	962,5
0,0	100,0	1,1	353,9	918,9

It is interesting to observe the sound speed trend for gas according to the variation in density of the mixture and so that the sound speed increases with decreasing in density. In addition, must be highlighted how speed of sound values are not largely affected by initial pressure and mixture concentrations, increasing methane fraction.

Figure 24 might help in better understanding what has been introduced earlier discussing relative pressure plots. It can be noticed that the intersection between flame velocity and speed of sound for 100 % H_2 fuel concentration occurs among photodiode 2 and photodiode 3. In this case it agrees with what was earlier announced for relative pressure plots.

Speed of sound considered in this case is the one present in Table 4 (C1 = 1090,4 m/s) since it better represents the conditions of the current experiment.

What was introduced earlier for TEST 2 (10 % CH_4 – 90 % H_2; 1.1 bar), analysing the relative pressure graphs, also finds a good match in Figure 22. In fact, the DDT in Figure 20 occurred around sensor 3, as the 5 bar threshold is exceeded at this distance by the ignition spark. In the figure below, it is clearly visible that the intersection between the flame velocity and the speed of sound (C2 = 1062.2 m/s) is located in the vicinity of sensor 3.

DDTs for increasing methane fraction values are visible in Figure 24. It is possible to underline, once again, that DDT distance from spark ignition (run-up distance) increases with increasing methane fraction.

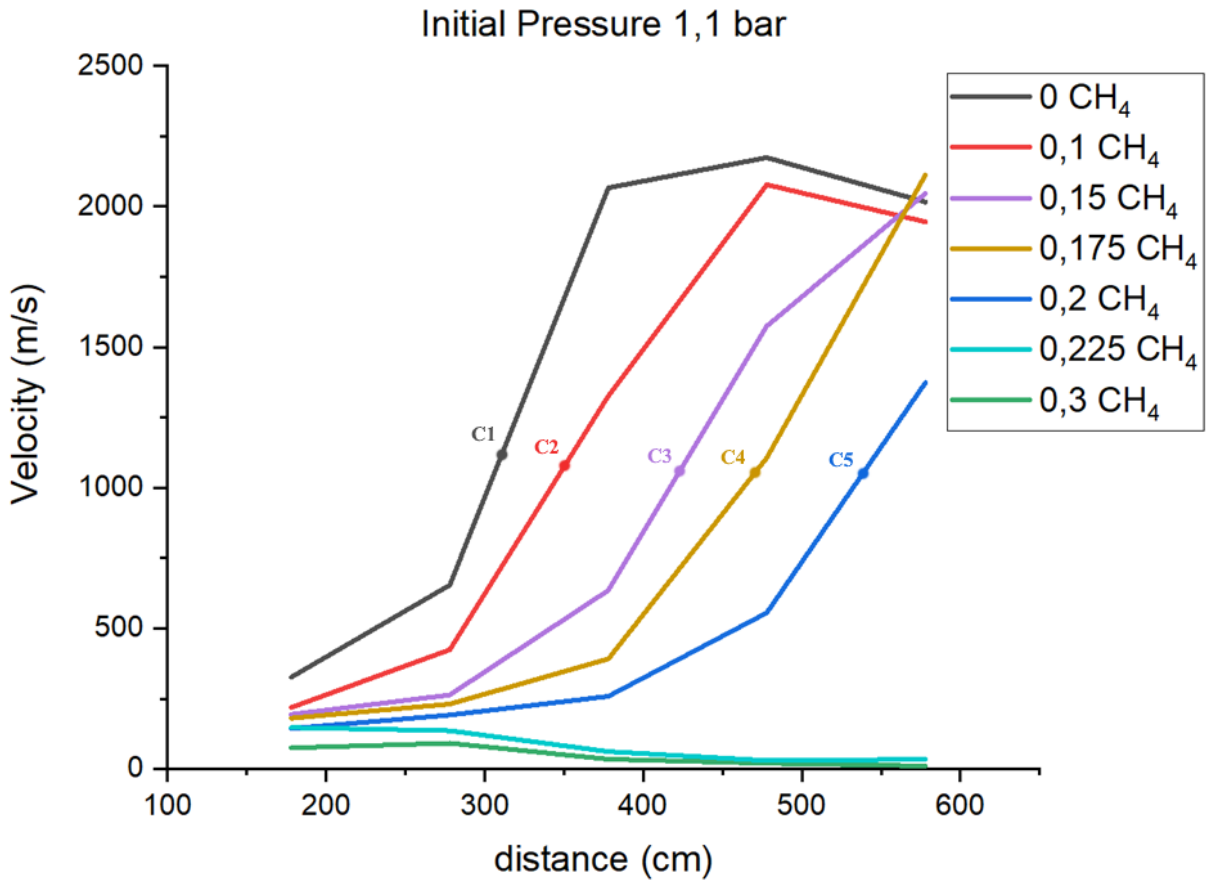

Figure 24 - Velocity plot compared with speeds of sound for 1,1 bar Initial Pressure

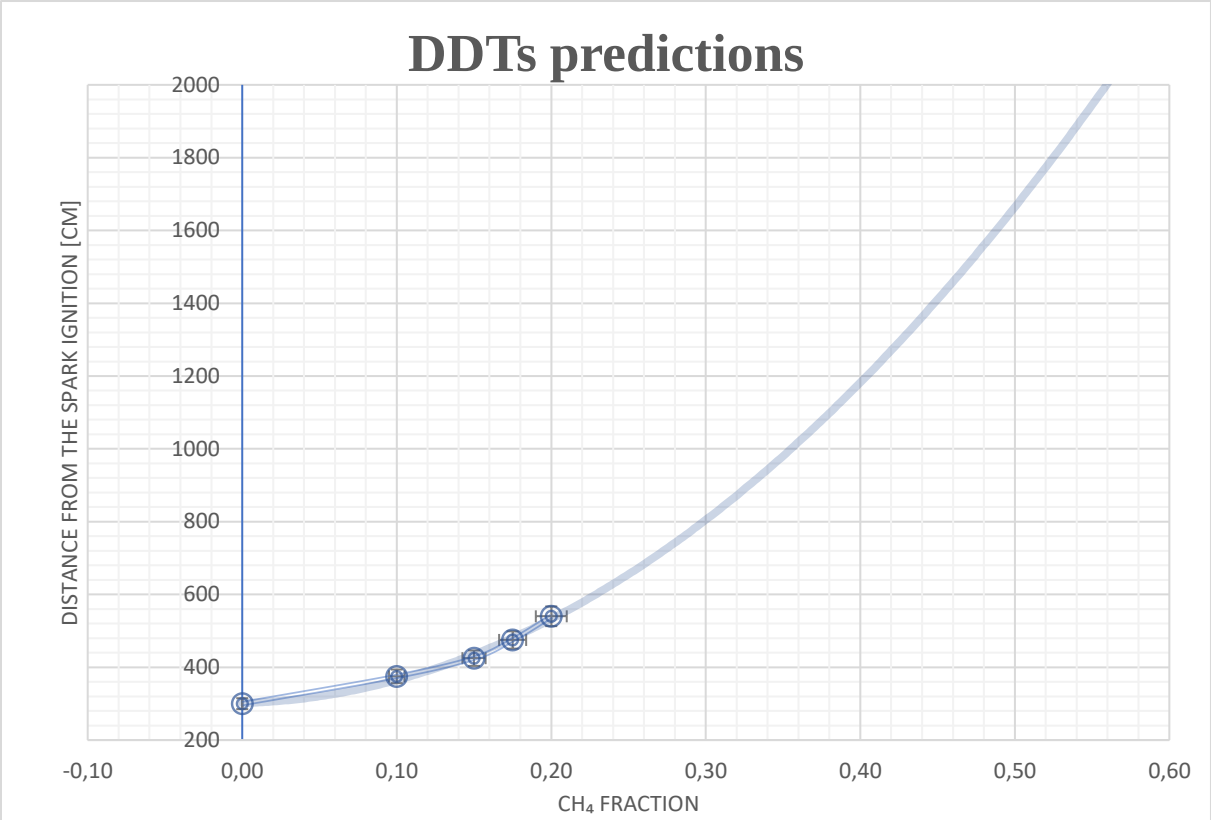

Figure 25 - DDTs predictions considering CH_4 fraction and distance from the spark ignition (initial pressure 1,1 bar)

Figure 25 shows the possible DDTs in a closed tube for higher methane fractions than that plotted in Figure 24. The curve in the graph above was obtained from the data in Figure 24, showing on the x-axis the methane fraction and on the y-axis the distance to the ignition spark where the transition from deflagration to detonation occurred. A prediction was then made, extending the trend shown.

It is known from the results previously shown in this work that it is not possible to achieve the transition from deflagration to detonation with methane fractions greater than 0.2 and with the specific conditions adopted in this experiment, such as the initial pressure of 1.1 bar, the length of the tube, the shape of the tube, etc. In fact, this can occur considering an ideal case, or a case using a different type of ignition. Therefore, in the case of a possible DDT, an idea of where the transition might take place can be made by looking at the graph above.

4.6. VELOCITY PLOT – INITIAL PRESSURE 1,5 BAR

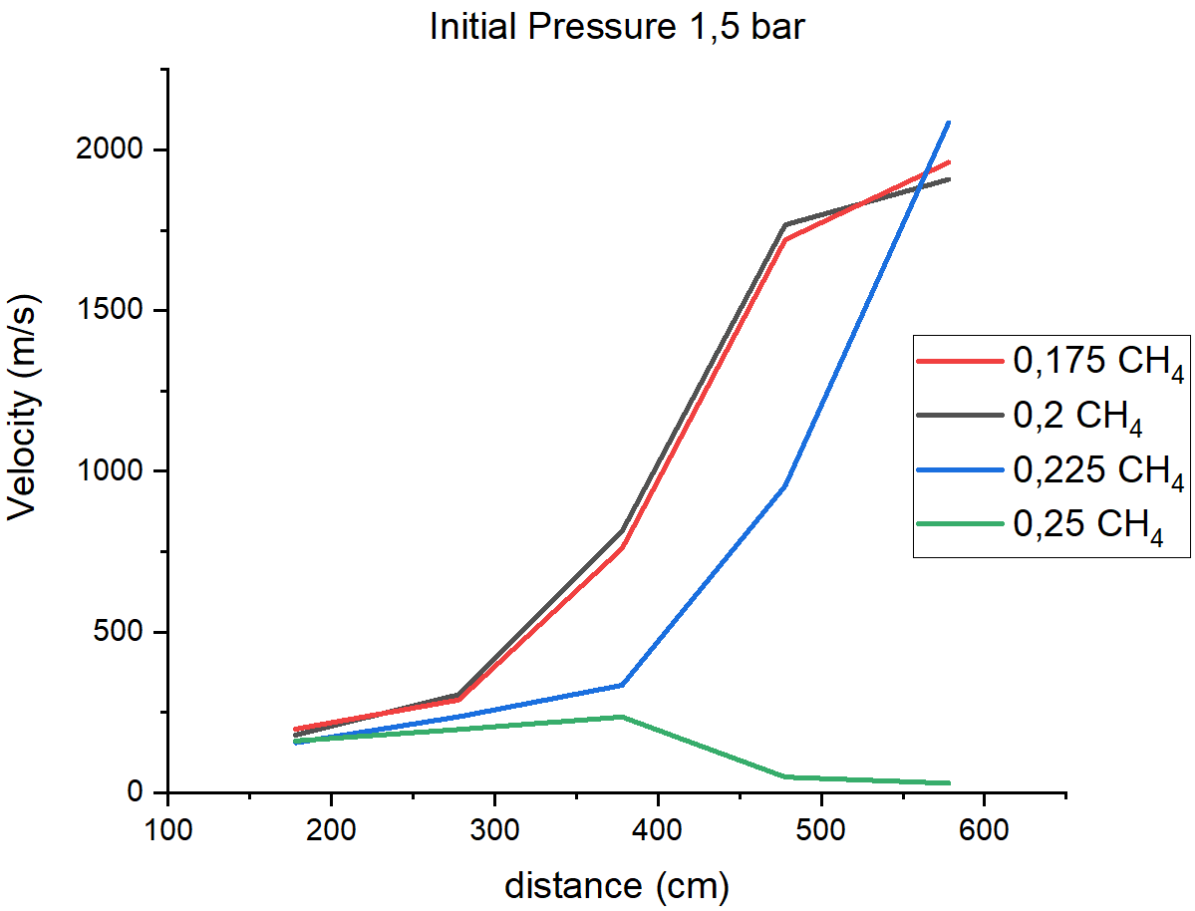

Figure 26 - Velocity plot for an initial pressure of 1,5 bar

Figure 26 shows the flame velocity graph for an initial pressure of 1.5 bar. As introduced above, the tipping point has shifted between methane fractions 0.225 and 0.25, while for lower pressures it lies between 0.2 and 0.225.

Again, looking at the graph, it can be assumed that the run-up distance increases with increasing methane fraction.

From this initial pressure value onwards, up to the highest initial pressure value established in the tests, the tipping point does not change. This means that the influence of pressure, apart from values below 1.5 bar, no longer affects the positioning of the DDT.

4.7. VELOCITY PLOT – METHANE FRACTION 0,20 AND 0,225

What has been said about the influence of pressure is also confirmed and visible in the graphs below, where the methane fraction was kept constant and the initial pressure varied to obtain the flame velocity diagrams.

In fact, for initial pressure values such as 1.1 bar and 1.3 bar, the run-up distance decreases with increasing initial pressure, and this is clearly visible in figure 27.

For higher pressure values, the influence is not so pronounced, as the trends shown for 1.5 bar, 1.7 bar and 1.9 bar are almost identical.

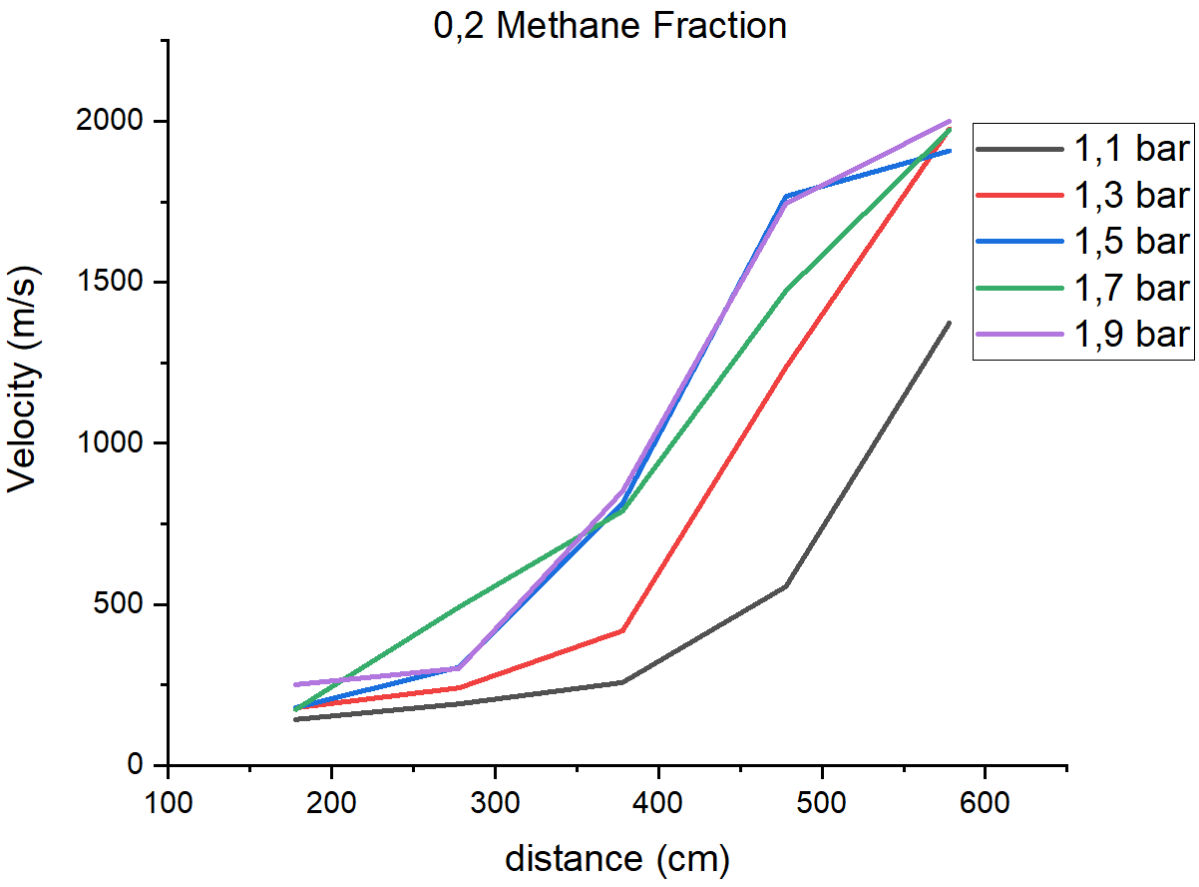

Figure 27 - Velocity plot for a 0,2 methane fraction

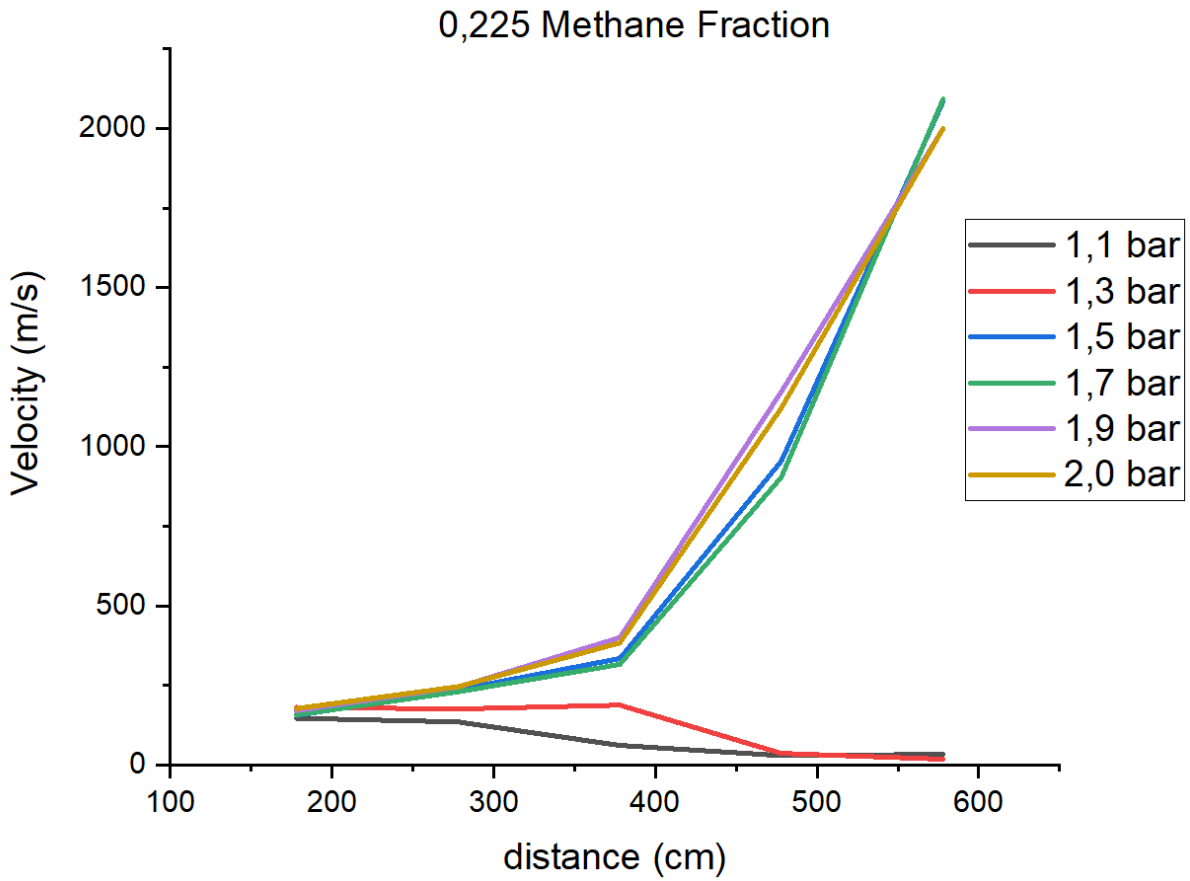

Figure 28 - Velocity plot for a 0,225 methane fraction

In Figure 28, the effect of pressure on the run-up distance is again shown, in fact for values above 1.3 bar the trends presented are almost identical. Furthermore, it is also shown that DDT occurs at 1.5 bar and not at 1.1 bar or 1.3 bar as in the previous case (Figure 27).

4.8. DDT IN AN OPEN TUBE

Further experiments were carried out in an open tube and a comparison with the results obtained for a closed tube is presented. To do this, a plastic membrane was placed on the outlet side, 623 cm from the spark ignition. In this way, the mixture was let out of the tube after ignition, breaking this plastic membrane. The tests were carried out at atmospheric pressure, and therefore with a good approximation, the data can be compared with the results obtained for the tube near initial pressure of 1,1 bar. All the performed tests for a closed tube are visible in Appendix B.

Interesting results were obtained because the tipping point moved between 0.325 methane fraction and 0.35 methane fraction while for a closed pipe and 1.1 bar initial pressure, it was placed between the methane fraction of 0.2 and 0.225.

It can be assumed that for longer tubes, the tipping point DDT would be moved even further away from ignition of the spark, but this will be better studied with future experiments.

Table 6 - Comparison between results obtained for a closed tube and results obtained for an open tube

Distance from the ignition	353 cm	403 cm	553 cm	603 cm	178 cm	278 cm	378 cm	478 cm	578 cm
	P3 (bar)	P4 (bar)	P5 (bar)	P6 (bar)	V1 (m/s)	V2 (m/s)	V3 (m/s)	V4 (m/s)	V5 (m/s)
0% CH_4 (C)	69	37			326	654	2066	2174	2016
0% CH_4 (O)		49	75	48	263	560	2264	2186	1979
10% CH_4 (C)	15	38	71	50	219	424	1326	2078	1946
10% CH_4 (O)		15	67	44	195	322	960	2008	2045
15% CH_4 (C)			95	126	194	263	635	1575	2047
15% CH_4 (O)			92	46	185	222	578	1491	2058
17,5% CH_4 (C)			139	99	180	230	391	1107	2112
17,5% CH_4 (O)			62	49				1542	2008
20% CH_4 (C)			55	135	143	192	258	556	1374
20% CH_4 (O)			88	48	142	222	548	1263	2082
22,5% CH_4 (O)			116	44				1240	2193
25% CH_4 (O)				85				906	1961
30% CH_4 (O)				18				465	1022
32,5% CH_4 (O)				23				612	1114

According to Table 6, another difference between the two different configurations is the pressure values recorded by piezoelectric sensors. In fact, the peak pressure values recorded for the closed pipe are much higher than those recorded for the open pipe. This is probably

due to the strong compression present in the closed tube between the flame and the outlet, which is not seen for the open tube since the mixture is allowed to leave the tube by breaking the membrane.

In Figure 29, the test with a methane fraction of 0.2 to 1.1 bar is visible for the closed tube and compared with the test carried out under the same initial conditions but in an open tube (Figure 30). Interesting differences in the two relative pressure trends can be observed. For the closed pipe there is a deflagration while, in the same conditions in an open pipe, there is with all probability a 100 % DDT.

The trend presented for TEST 15 (Figure 29; Figure 23) is the typical pressure graph obtained for deflagration, regardless of the initial conditions, and shows that all the pressure values recorded by the sensors are very similar to each other. This highlights the uniformity of the pressure inside the pipe probably due to the lack of ability of the mixture to achieve a sufficient speed to reach the transition point.

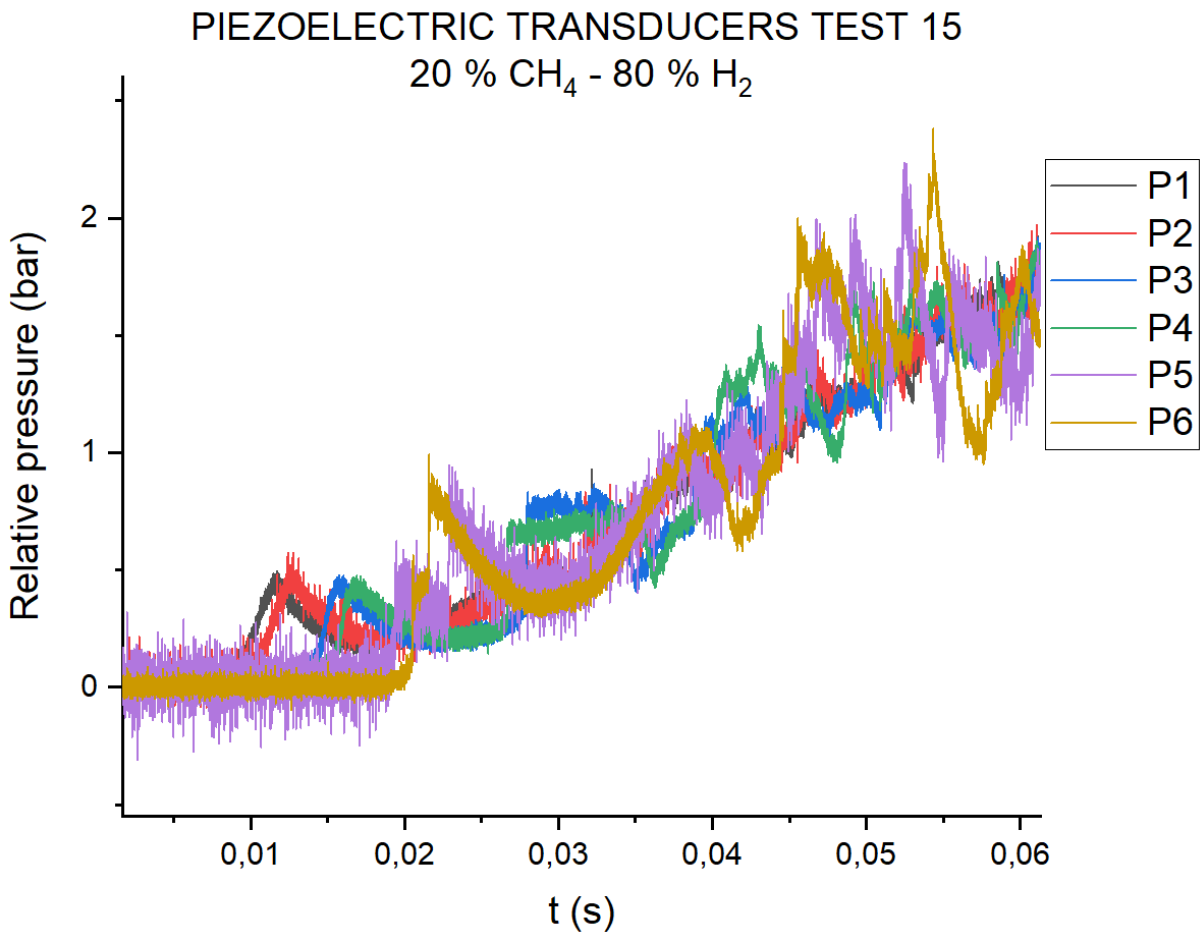

Figure 29 - Enlarged TEST 15 relative pressure plot (20 % CH_4 and 1,1 bar)

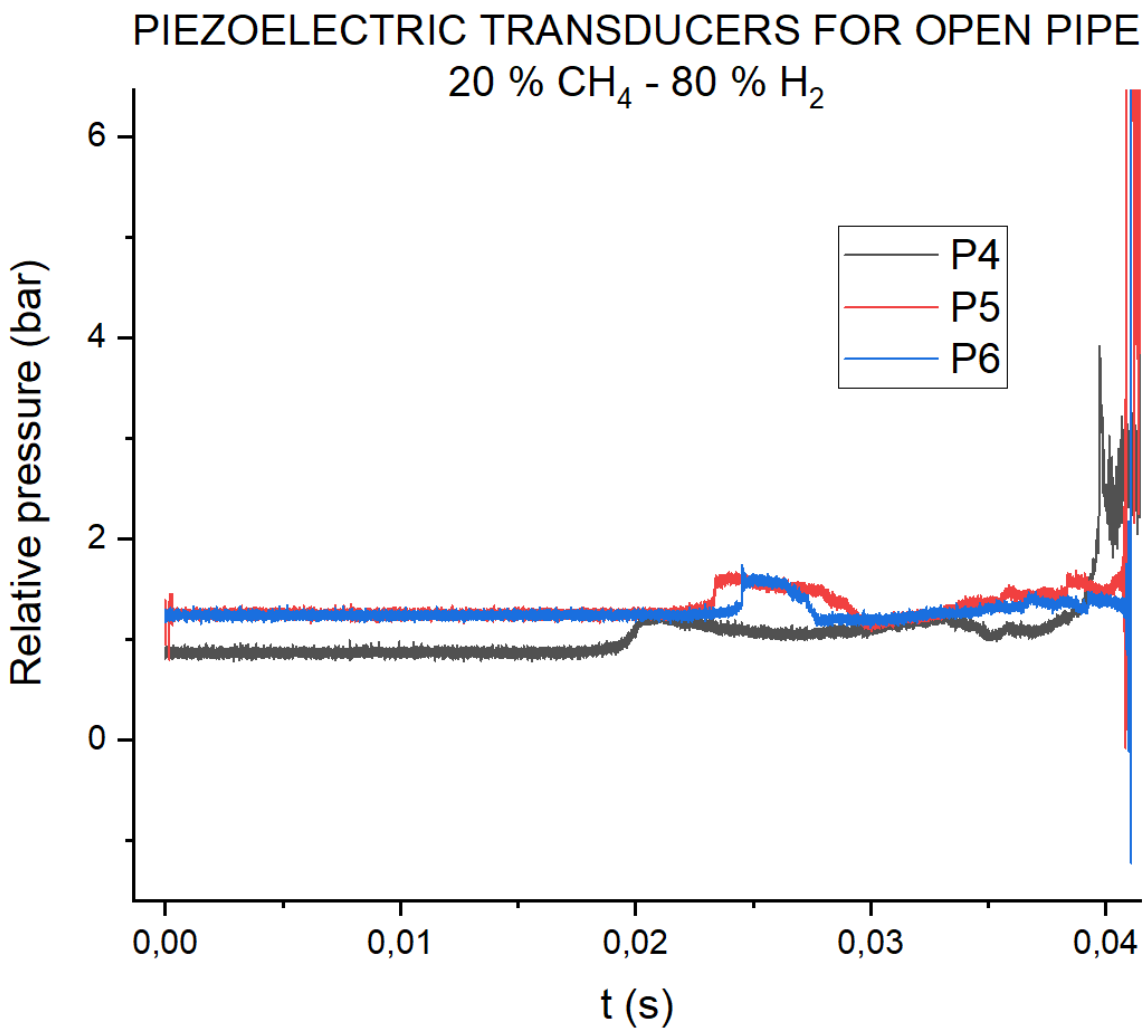

Figure 30 - Enlarged relative pressure plot for an open pipe, TEST 135 (20 % CH_4; 1,1 bar)

On the other hand, Figure 30 shows a different trend for the relative pressure in an open pipe (TEST 135, 20 % CH_4 and 1,1 bar), especially with regard to the initial fractions of time, where the pressure does not seem to be affected by the stagnation of pressure from the exit side of the pipe. Thus, the mixture is able to reach a sufficient velocity to reach the transition point and thus detonation conditions.

Figure 31 shows a comparison of the possible DDT in an open and closed pipe for higher methane fractions than those presented in Table 6. The slope of the curve for the open pipe case is lighter than that presented for the closed pipe experiment, probably due to the lack of pressure stagnation in the outlet side of the pipe.

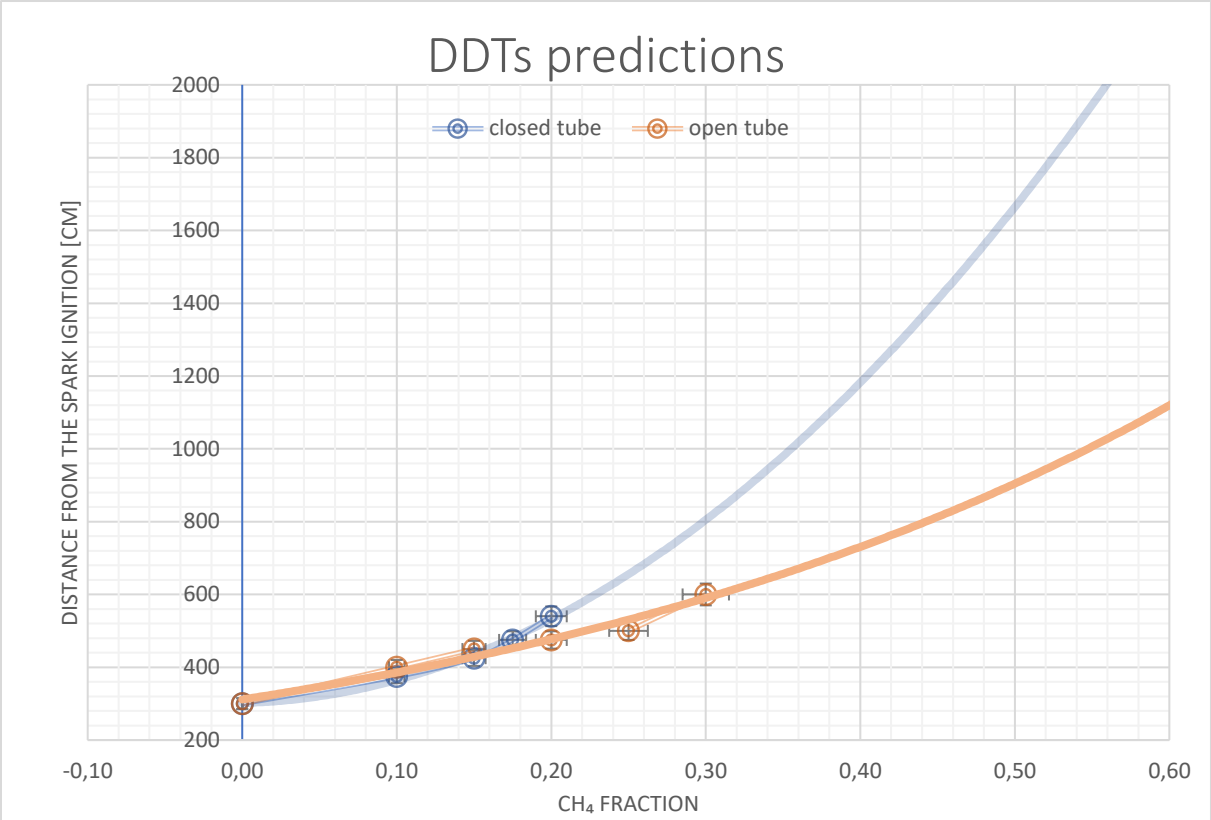

Figure 31 - DDTs predictions considering CH4 fraction and distance from the spark ignition in an open and closed pipe (initial pressure 1,1 bar)

5. FAILURES AND DEFECTS

In this section, problems and failures that occurred during the experience have been reported to make things easier for people that want to reproduce this kind of experiment.

5.1. INTERNAL PRESSURE

To avoid internal system and device failure, the maximum initial pressure allowed was 2 bar. This precaution was not sufficient to prevent the system from breaking down.

Initially, it was possible to adjust the initial pressure to the desired value, since once valve number 3 in Figure 13 was closed, no further pressure loss occurred.

After a few tests, the effect of the valve began to diminish and adjusting the initial pressure to the desired value became increasingly difficult.

Many inspections focused our attention on the valve at the end of the pipe (Figure 14). The valve seal had to be replaced because it had been irreversibly damaged by the succession of detonations and was therefore no longer able to prevent pressure loss.

This problem was one of the main contributors to the errors in the entire experiment.

Figure 32 shows the inside of the valve at the time of replacement.

Figure 32 - Damaged valve seal

5.2. DIODES AND PIEZOELECTRIC TRANSDUCERS FAILURES

Numerous failures of the diodes and piezoelectric transducers occurred during the entire process. The only two broken piezoelectric sensors were numbers 5 and 6, as the detonation occurred mainly in their vicinity. Probably, due to the high intensity of the explosion, either the crystal inside the diode or the protective membrane was irreversibly damaged and, due to the high cost, was not replaced.

As for the diodes, they too failed several times and not only those in position number 5 or 6, but in this case, they were repaired or replaced. In fact, a diode can be bought for a few cents, while piezoelectric transducers can cost up to 1,200 euros a piece.

This is why some of the pressure and speed graphs show missing values, and this is because the broken sensors were not able to measure and record the correct value.

In order to have complete velocity graphs, experiments with missing velocities were repeated several times to present a better comparison.

Figure 33 shows a burnt-out diode, which was immediately replaced.

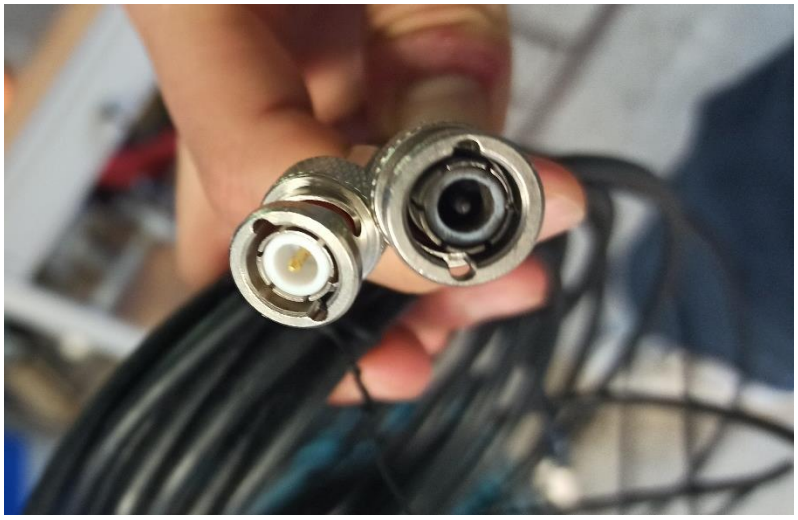

Figure 33 - Burnt diode number 5

5.3. SPARK IGNITION THRESHOLD VOLTAGE

As already mentioned, the ignition signal was given by an electronic timer set to 0.5 seconds and connected to an ignition cage and the BENCH software via two different wires. Once the timer button was pressed, a spark was generated and the mixture ignited. At the same time, the programme received a signal to start recording the values transmitted by the sensors.

The main problem with this component was the threshold voltage of the ignition cage, which was initially set at 0 V. Sometimes, due to the numerous oscillations and vibrations, this threshold value was exceeded even without pressing the button, causing the mixture to ignite but not the programme to run, thus losing all data of the current experiment.

For this reason, the two wires connecting the ignition cage to the tube were placed in the correct position only a few seconds before the start of the experiment, in order to avoid unwanted ignitions.

In addition, the ignition trigger value was increased so that the slightest oscillation or vibration would not be able to produce an unwanted self-ignition. Initially, the value was increased to 100 mV, but due to delays (approx. 1 second) in data recording, it was reduced to 20 mV. It was possible to change this value via the BENCH software settings.

An additional trick used was to insert two transformers, placed before the ignition cage and the software, in order to clean the voltage signal as much as possible and limit the effect of oscillations and vibrations. (Figure 34)

Figure 34 - Transformer interposed between the BENCH software and the electronic-timer

5.4. INTERNAL TEMPERATURE SENSOR

This sensor allows the operator to control the temperature value inside the pipe, not because this parameter is being studied, but as a matter of homogeneity of the initial conditions of each experiment. Therefore, in the event that the temperature inside the pipe was too different from the ambient temperature (20 °C), this was modified by varying the value of the heating cable (warm-up cable), so that all experiments were carried out with a more or less similar initial temperature.

After about 100 experiments, this sensor also failed because the metal wire capable of detecting the internal temperature broke.

In Figure 35 it is possible to see the cut wire, which should instead protrude about two cm from the surface of the nut.

The damaged nut was then replaced and the sensor restored.

Figure 35- Broken internal temperature sensor

5.5. THE MASS FLOW

Initially, the total mass flow rate of the three species (methane, hydrogen and air) at the pipe inlet was to be 30 L/min, but since the hydrogen and methane vessels had a flow rate of 50 L/min and 10 L/min respectively, this value was doubled to 60 L/min. This ensured better accuracy, because increasing the flow per minute required less accuracy from the mixture preparation system, as more adequate quantities were required depending on the size of the vessels, especially for the hydrogen one.

6. SIMULATIONS

Through the ANSYS simulator, using the CHEMKIN package, the flame velocity of the mixture was calculated and then compared with the experimental value obtained through testing. The KIBO chemical kinetics mechanism, developed at the University of Bologna, was used.

The aim of this comparison was to see if there is a correlation between the values obtained experimentally and those calculated through the simulations.

Obviously, one does not expect to obtain the same results, as the experimental route is subject to numerous contingencies and losses, while the simulation results are performed considering an ideal route. What is expected is to see a common laminar combustion velocity trend and correlation between all different cases and mixtures.

Without knowing whether a mixture has detonated or simply deflagrated after ignition, by looking at the diagram of the velocities obtained from the diodes, it is possible to predict the end result simply by seeing whether the velocities are above or below the value of the speed of sound in the same mixture. If the velocities obtained by the diodes exceed the speed of sound, then DDT has occurred. This is due to turbulence and all the effects it causes, such as increased overpressure, etc. The isobaric speed of sound for each mixture can be obtained in two different ways. Either through the ANSYS simulator or by using the GASEQ equilibrium software. The results obtained in both cases are very similar.

One cannot expect similar numerical results between reality and simulation because many conditions are different. The main problem is that the laboratory tests were performed in a closed tube, so both ends were sealed. This means that the inlet velocity of the mixture immediately before ignition is 0 m/s. On the other hand, the simulator needs an inlet velocity other than 0 m/s to work, and this is because the simulations are performed in an open tube.

This leads to a huge difference in numerical terms between the values obtained experimentally and those obtained through simulations, which is why the aim of the simulation is to find a correspondence in conceptual terms.

The Flame-speed Calculator was used to build the simulation model. This component simulates a freely propagating flame and is suitable for detecting uniquely deflagrations. For this reason, the mixture containing 100 per cent methane as fuel was considered, since it is known from the experiment that this is a case of deflagration.

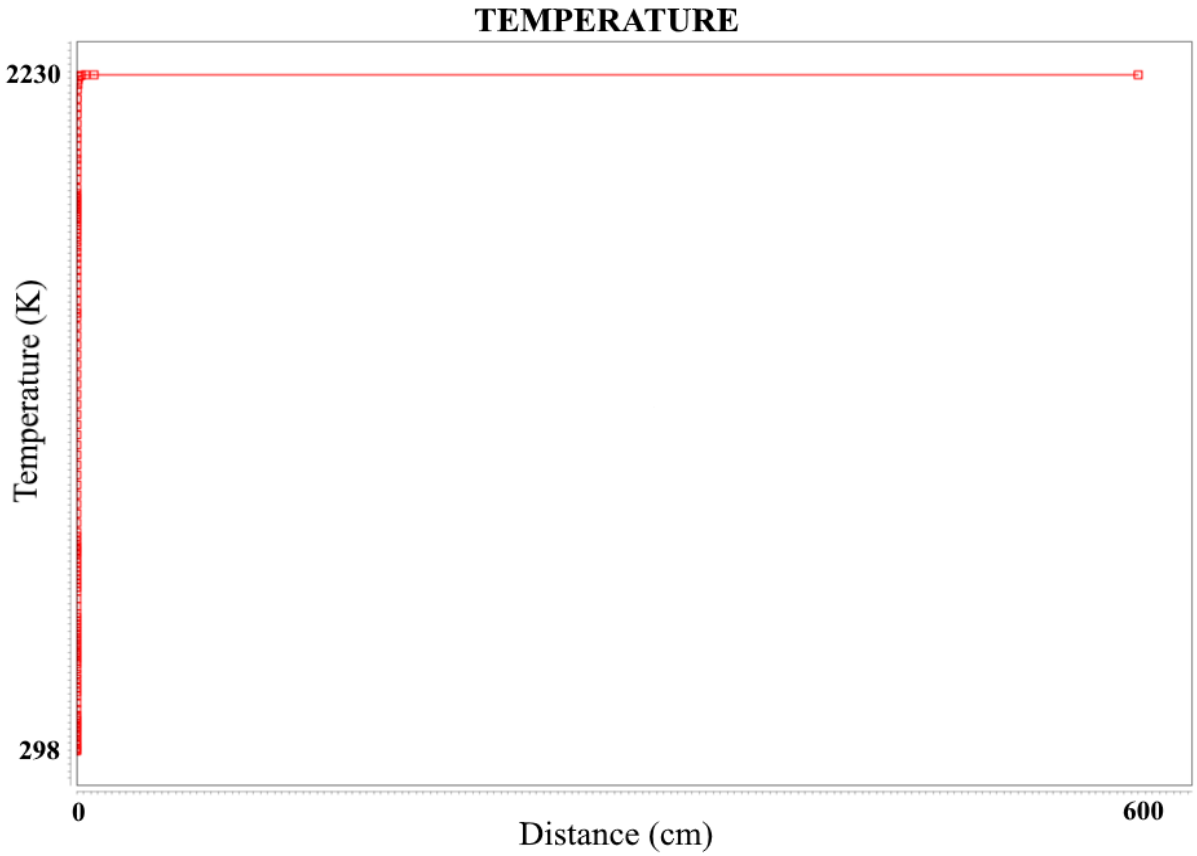

Figure 36 - Temperature obtained through ANSYS simulator

The simulator provides values for the temperature of the mixture, before and after combustion, the speed of sound in both the burnt and unburnt medium and the flame speed. The latter value must be multiplied by an expansion ratio that takes into account the acceleration provided by the expansion of the burnt gases. Since the pressure value along the simulation is constant at 1,1 bar, the expansion ratio is given by the ratio of the temperature of the burnt gases to that of the unburnt gases.

In this case, the expansion ratio is 7.48 since, looking at the temperature graph above, the temperature values before and after combustion are 298 k and 2230 k respectively. (Figure 36)

The expansion ratio must be multiplied by the axial velocity obtained after combustion (Sb) which is 2.66 m/s (Figure 37). The final result is 19.9 m/s and is comparable to the value obtained during the experiments for a mixture 100 % CH_4 and initial pressure of 1,1 bar. In the graph shown in Figure 38, it can be seen that at the centre of the tube, the velocity is almost 19 m/s. Since the speed of sound of the combustion products has the same value as that recorded in Table 5 (ideal case) for a 100 per cent CH_4 mixture, i.e. 918.9 m/s, it can be stated once again that DDT does not occur.

In this deflagration case, the comparison of the data obtained in the two different cases shows some similarities in numerical terms, although there are important differences between the setup of the experimental case and that of the simulation.

It is not the same for the detonation cases, as the setup used for the simulation is not the most suitable for detecting the detonation phenomenon.

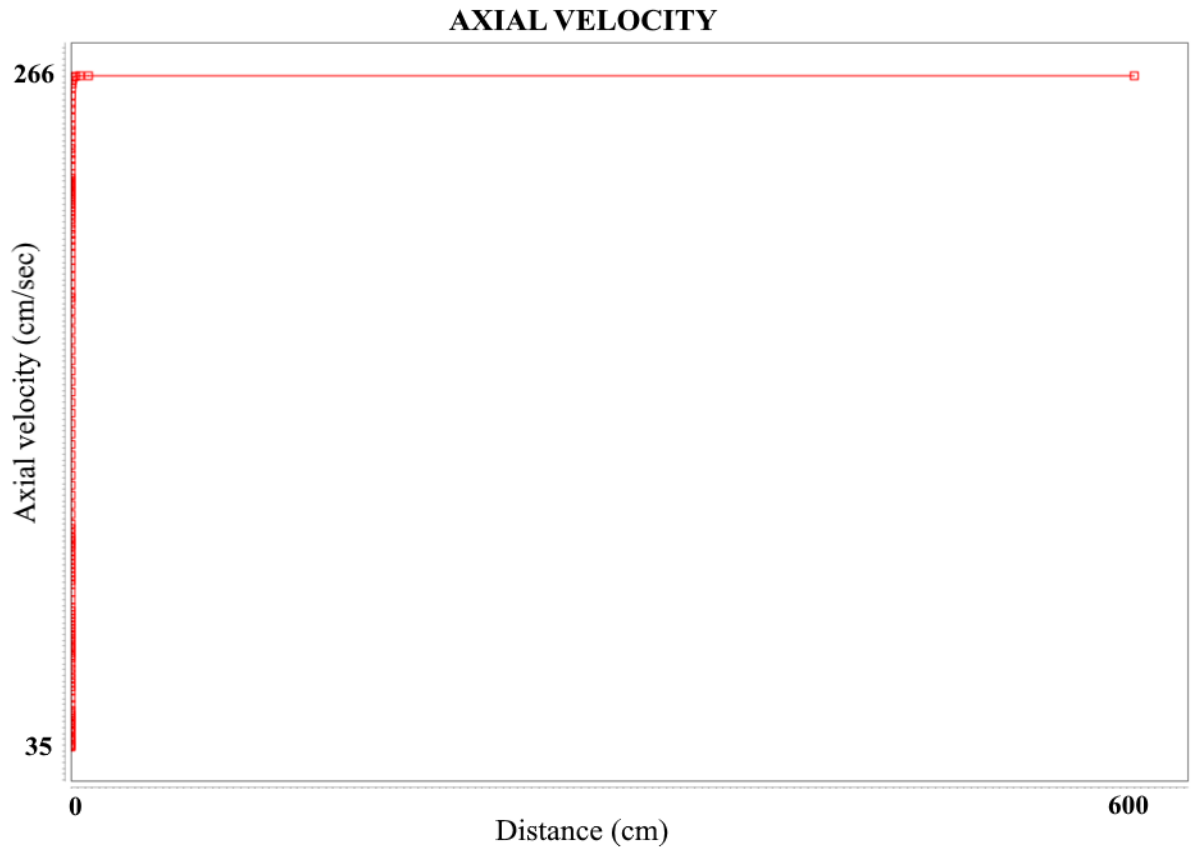

Figure 37 - Axis velocity obtained through ANSYS simulator

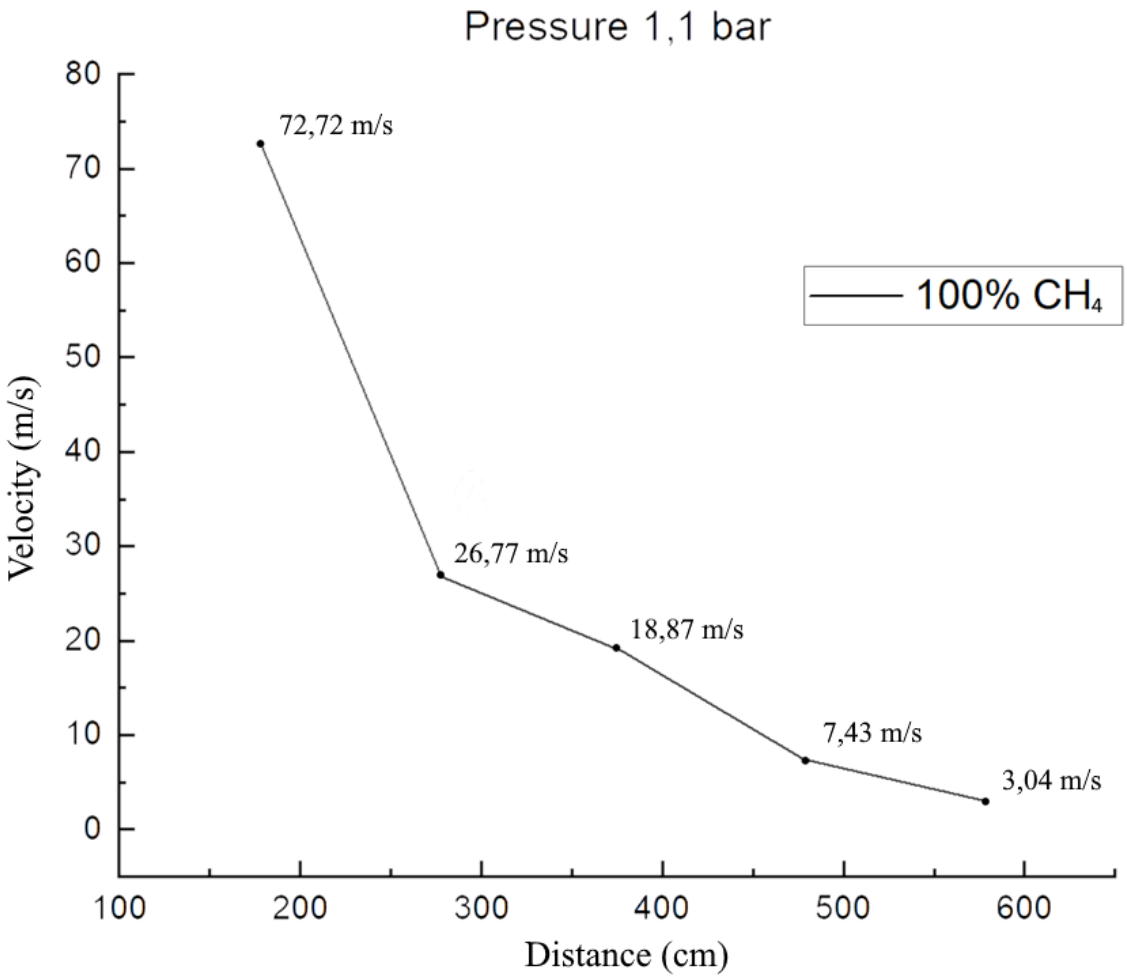

Figure 38 - Velocity plot TEST 12 (100% CH_4; Initial Pressure 1,1 bar)

CONCLUSIONS

In this paper, deflagration-to-detonation transition (DDT) of stoichiometric hydrogen-methane-air mixtures were investigated in an unobstructed circular steel tube with a diameter of 50 mm and 6.23 m length. The tube was closed on both sides. The probability of DDT was detected as a function of initial conditions such as absolute pressure and hydrogen and methane concentrations. The initial pressure was varied from 1.1 to 2 bar, while the fuel fraction was varied from 100 % H_2 to 100 % CH_4. To measure relative pressure and flame velocity of the mixture, six photodiodes and six piezoelectric sensors were installed along the tube, and a high-voltage induction spark was used as the ignition source.

It has been observed that the transition from deflagration to detonation occurs mainly around values of 80 % hydrogen and that an increase in pressure leads to a lower hydrogen-to-methane ratio capable of detonating in unobstructed pipes. In fact, it has been seen that the tipping point lies between a methane fraction of 0.2 and 0.225 for pressure values up to a maximum of 1.3 bar. For values above 1.3 bar, the tipping point is between the methane fraction of 0.225 and 0.25 and is no longer affected by the pressure increase.

Furthermore, the results of the experiment show that the distance to the ignition spark, at which the transition from deflagration to detonation occurs (run-up distance), for a given pressure value, increases with increasing methane fraction. To better observe the DDT distance, observations and comparisons were made on both the relative pressure and flame velocity graphs, identifying with a good margin of error the possible distances at which the transition could occur.

In the flame speed graphs, the transition occurs when the flame speed exceeds the speed of sound for that specific mixture. The results show that for mixtures with a hydrogen fraction of 100 per cent, this occurs between sensor 2 and sensor 3, i.e. about 300 cm away from the ignition spark. This distance value increases with increasing methane fraction, since for tests performed with 90 % H_2 and 10% CH_4, the transition point is around sensor 3 (350 cm). These results were in good agreement with the wave pressure values recorded during the experiments. Predictions and results for further fuel concentrations were presented.

A comparison with experiments conducted in an open pipe under the same initial conditions was then presented. In this case, the tipping point shifted between a methane fraction of 0.325 and 0.35, and the comparison of the predicted DDT curves showed a gentler slope for the open pipe case, probably due to the lower pressure present at the outlet side of the pipe.

REFERENCES

[1] DVGW (2021). Wasserstoff-Beimischung - Sicherheit in Ihrem Zuhause. Online available under: https://www.dvgw.de/medien/dvgw/leistungen/publikationen/sicherheit-h2-beimischung-dvgw.pdf

[2] Lowesmith BJ, Mumby C, Hankinson G, Puttock JS. Vented confined explosions involving methane/hydrogen mixtures. Int J Hydrogen Energy 2011; 36(3):2337-43

[3] Lowesmith BJ, Hankinson G, Johnson DM. Vapour cloud explosions in a long congested region involving methane/hydrogen mixtures. Process Saf. and Environ. Prot. 2011, 89, 234-247.

[4] Shirvill LC, Roberts TA, Royle M, Willoughby DB, Sathiah P. Experimental study of hydrogen explosion in repeated pipe congestion – Part 2: Effects of increase in hydrogen concentration in hydrogen-methane-air mixture. Int. J. Hydrogen Energy 2019, 44, 3264-3276.

[5] Qiuju Ma, Qi Zhang, Jiachen Chen, Ying Huang, Yuantong Shi. Effects of hydrogen on combustion characteristics of methane in air. Int. J. Hydrogen Energy 2014, 39, 11291-11298.

[6] Salzano E, Cammarota F, Di Benedetto A, Di Sarli V. Explosion behavior of hydrogen-methane/air mixtures. J. Loss Prev. Process Ind. 2012, 25, 443-447.

[7] Porowski R, Teodorczyk A. Experimental study on DDT for hydrogen-methane-air mixtures in tube with obtacles. Journal of Loss Prevention in the Process Industries 2013, 26, 374-379.

[8] Zhang Bo, Pang Lei, Gao Yuan. Detonation limits in binary fuel blends of methane/hydrogen mixtures. Fuel 2016, 168, 27-33.

[9] Zhang Bo, Pang Lei, Shen Xiaobo, Gao Yuan. Measurement and prediction of detonation cell size in binary fuel blends of methane/hydrogen mixtures. Fuel 2016, 172, 196-199.

[10] Wang Lu-Qing, Ma Hong-Hao, Shen Zhao-Wu, Chen Dai-Guo. Experimental study of DDT in hydrogen-methane-air mixtures in a tube filled with square orifice plates. Process Saf. Environ. Prot. 2018, 116, 228-234.

[11] Middha Prankul, Engel Derek, Hansen Olav R. Can the addition of hydrogen to natural gas reduce the explosion risk?. Int. J. Hydrogen Energy 2011, 36, 2628-2636.

[12] Wierzba I, Ale BB. Rich flammability limits of fuel mixtures involving hydrogen at elevated temperatures. Int. J. Hydrogen Energy 2000, 25, 75-80.

[13] Askar Enis, Volkmar Schröder, Schütz Stefan, Seemann Albert. Power-to-Gas: Safety Characteristics of Hydrogen/Natural-Gas Mixtures. Chemical Engineering Transactions 2016, 48, 397-402.

[14] Chaumeix N, Pichon S, Lafosse F, Paillard C.-E. Role of chemical kinetics on the detonation properties of hydrogen/natural gas/air mixtures. Int. J. Hydrogen Energy 2007, 32, 2216-2226.

[15] Cadorin Margherita, Morini Mirko, Pinelli Michele. Numerical analysis of high Reynolds number flow of high pressure fuel through rough pipes. Int. J. Hydrogen Energy 2010, 35, 7568-7579.

[16] Bull D.C, Elsworth J. E, Shuff P. J. Detonation Cell Structures in Fuel/Air Mixtures. Combustion and Flame 1982, 45, 7-22.
[17] Ciccarelli G, Ginsberg T, Boccio J, Economos C, Sato K, Kinoshita M. Detonation Cell Size Measurement and Predictions in Hydrogen-Air-Steam Mixtures at Elevated Temperatures. Combustion and Flame 1994, 99, 212-220.
[18] Ciccarelli G, Boccio J.L, Ginsberg T. The influence of initial temperature on flame acceleration and deflagration-to-detonation transition. Twenty-Sixth Symposium on Combustion 1996, 2973-2979.
[19] Mahajan D, Tan K, Venkatesh T, Kileti P, Clayton C.R. Hydrogen Blending in Gas Pipeline Networks – A Review. Energies 2022, 15, 3582.
[20] Chemical Equilibrium with Applications (CEA, available from the NASA Glenn Research Center at http://www.grc.nasa.gov/WWW/CEAWeb/).
[21] The Detonation Phenomenon. John H. S. Lee. 2008, Cambridge.

APPENDIX A

Tests performed for the closed tube configuration

TESTS		H_2	CH_4	Air	waiting	Initial pressure	Methane fraction	Detonation probability
		%	%	%	time	bar		%
test 117, 118	test 1	29	0	71	10 min	1,1	0,000	100
	test 2	21,99633	2,43293	75,57074	10 min	1,1	0,100	100
test 46, 48, 49, 114	test 47	19,02301	3,35112	77,62588	10 min	1,1	0,150	80
test 56, 57	test 55	19,05318	3,36723	77,5796	10 min	1,3	0,150	100
test 51, 52, 53, 54, 115	test 50	17,77555	3,76855	78,45589	10 min	1,1	0,175	50
test 101, 102, 104	test 103	17,74516	3,76918	78,48566	10 min	1,3	0,175	100
test 62, 63, 64	test 123	17,78333	3,76667	78,45	10 min	1,5	0,175	100
test15, 16, 68, 69, 70, 116	test 3	16,60277	4,13402	79,26321	10 min	1,1	0,199	14,3
test 21, 22, 105, 112, 113	test 20	16,58333	4,13333	79,28333	10 min	1,3	0,200	50
test 24,25,90,91,127	test 23	16,58333	4,13333	79,28333	10 min	1,5	0,200	80
test 83, 84 ,85	test 82	16,60554	4,13471	79,25975	10 min	1,7	0,199	100
test 65, 66, 67	test 119	16,59447	4,13196	79,27358	10 min	1,9	0,199	100
test 106, 107	test 108	15,52184	4,51817	79,95999	10 min	1,1	0,225	0
test 110, 111	test 109	15,53074	4,51591	79,95334	10 min	1,3	0,225	0
test 87, 88, 89	test 86	15,51667	4,5	79,98333	10 min	1,5	0,225	75
test 92, 93, 94, 120	test 124	15,51925	4,51742	79,96333	10 min	1,7	0,225	100
test 95, 96, 97	test 121	15,54223	4,51441	79,94336	10 min	1,9	0,225	100
test 98, 99, 100	test 122	15,51408	4,51591	79,97	10 min	2	0,225	100
test 74, 75, 76	test 125	14,4739	4,81908	80,70702	10 min	1,5	0,250	0
test 78	test 77	14,48575	4,81747	80,69678	10 min	1,7	0,250	0
test 58,59,60,61	test 126	14,4739	4,81908	80,70702	10 min	1,9	0,250	0
test 80, 81	test 79	14,47873	4,82068	80,70058	10 min	2	0,250	0
test 44, 45	test 43	13,53333	5,13333	81,33333	10 min	2	0,275	0
test 5	test 4	12,6063	5,4027	81,991	10 min	1,1	0,300	0
test 28, test 30	test 27	12,6021	5,4009	81,997	10 min	1,5	0,300	0
test 32, test 33	test 31	12,62508	5,4036	81,97131	10 min	1,7	0,300	0
test 39	test 38	12,62087	5,4018	81,97733	10 min	1,9	0,300	0
test 41, test 42	test 40	12,61051	5,4045	81,98499	10 min	2	0,300	0
	test 6	9,6032	6,40213	83,99466	10 min	1,1	0,400	0
	test 7	7,16667	7,16667	85,66667	10 min	1,1	0,500	0
	test 8	5,1842	7,8013	87,0145	10 min	1,1	0,601	0
	test 9	3,55237	8,33889	88,10874	10 min	1,1	0,701	0
	test 10	2,2	8,75	89,05	10 min	1,1	0,799	0
	test 11	1,03351	9,16819	89,7983	10 min	1,1	0,899	0
	test 12	0	9,4	90,6	10 min	1,1	1,000	0

APPENDIX B

Tests performed for the open tube configuration

TESTS		H_2	CH_4	Air	waiting	Initial pressure	Methane fraction	Detonation probability
		%	%	%	time	bar		%
test 132, 133	test 128	29,0058	0	70,9942	10 min	1,1	0	100
test 134	test 129	21,9912	2,43902	75,56977	10 min	1,1	0,100	100
test 145	test 131	19,0076	3,36134	77,63105	10 min	1,1	0,150	100
	test 146	17,78	3,78	78,44	10 min	1,1	0,175	100
test 135, 136	test 130	16,61329	4,1233	79,26341	10 min	1,1	0,199	100
	test 137	15,52932	4,5027	79,96798	10 min	1,1	0,225	100
	test 138	14,46	4,82	80,72	10 min	1,1	0,250	100
	test 139	12,64506	5,40216	81,95278	10 min	1,1	0,299	100
test 142	test 141	11,80708	5,68341	82,50951	10 min	1,1	0,325	100
test 143, 144	test 140	11,02	5,94	83,04	10 min	1,1	0,350	0